2

Conf-9208186--5

UCRL-JC-114583
PREPRINT

New relativistic S-matrix results for scattering - beyond the usual anomalous factors/beyond impulse approximation

R. H. Pratt [a], Lynn Kissel [b,a] and P. M. Bergstrom, Jr. [a,1]

[a]Department of Physics and Astronomy,
University of Pittsburgh, Pittsburgh, PA 15260 USA

[b] Computational Physics Group Lawrence Livermore
National Laboratory, Livermore, CA. 94550, USA

This Paper Prepared for Submittal to the
Proceedings of the ICAS Conference
August 17-21, 1992
Malente/Hamburg, Germany

August, 1993

Lawrence Livermore National Laboratory

This is a preprint of a paper intended for publication in a journal or proceedings. Since changes may be made before publication, this preprint is made available with the understanding that it will not be cited or reproduced without the permission of the author.

AUG 16 1993
OSTI

MASTER

DISTRIBUTION OF THIS DOCUMENT IS UNLIMITED

DISCLAIMER

This document was prepared as an account of work sponsored by an agency of the United States Government. Neither the United States Government nor the University of California nor any of their employees, makes any warranty, express or implied, or assumes any legal liability or responsibility for the accuracy, completeness, or usefulness of any information, apparatus, product, or process disclosed, or represents that its use would not infringe privately owned rights. Reference herein to any specific commercial products, process, or service by trade name, trademark, manufacturer, or otherwise, does not necessarily constitute or imply its endorsement, recommendation, or favoring by the United States Government or the University of California. The views and opinions of authors expressed herein do not necessarily state or reflect those of the United States Government or the University of California, and shall not be used for advertising or product endorsement purposes.

New relativistic S-matrix results for scattering - beyond the usual anomalous factors/beyond impulse approximation

R. H. Pratt,[a] Lynn Kissel[b,a] and P. M. Bergstrom, Jr.[a,1]

[a]Department of Physics and Astronomy, University of Pittsburgh, Pittsburgh, PA 15260, USA

[b]Computational Physics Group, L Division, Lawrence Livermore National Laboratory, Livermore, CA 94550, USA

Abstract

The relativistic second-order S-matrix elements for photon-atom scattering have been successfully calculated with numerical methods within the independent particle approximation (IPA). This permits an assessment of the validity of simpler approximate predictions which are commonly used and it offers the possibility of improved tabulations of theoretical predictions. A variety of unresolved issues remain, some associated with the relativistic theory, some with IPA.

The systematic use of the second-order S-matrix in calculations of Rayleigh scattering from isolated atoms has led to significant progress in understanding this process and to a wide range of agreement with experiment. The energy and angular dependence of anomalous factors and the importance of relativistic, higher- multipole and bound-bound contributions in their calculation is better understood. However correlation effects must also be included to obtain predictions for the near-edge region; such extensions of the present S-matrix calculation have been discussed but few results are sofar available. Existing empirical approaches can be assessed in regard to their success in dealing with known IPA features.

We have recently calculated the relativistic second-order S-matrix element for Compton scattering and have begun to try to understand this process in different regions. We can discuss when the more complete calculation confirms the standard Compton peak. In the softer part of the spectrum impulse approximation fails. There can be resonant Raman peaks, and in the soft-photon region the spectrum is infrared divergent, proportional to the photoeffect angular distribution. This means the traditional incoherent scattering factor is undefined in the absence of a low-energy detector efficiency cutoff.

---

[1] Present address: Theoretical Physics, The University of Tennessee, 200 South College, Knoxville, TN 37996-1501, USA.

1. INTRODUCTION

We wish to describe recent progress in the theoretical calculation of the amplitudes and cross sections for elastic and inelastic scattering of photons from atoms. We will also discuss the extent of agreement with experiment which has been achieved. This work is largely based on numerical calculations of the relativistic second-order S-matrix element in external-field quantum electrodynamics for photon-atom scattering within independent particle approximation. We restrict our consideration to incident photon energies below about 1 MeV, so that photon-atom scattering can largely be understood as scattering from the bound electrons of the atom. We also restrict our consideration to scattering from isolated atoms (or ions), thereby not dealing with the interesting and important additional features which arise in scattering from molecules, plasmas, surfaces and solids.

With these new results it is possible to discuss the validity of widely used simpler approaches to such calculations. For elastic (Rayleigh) scattering from bound electrons, such approaches have been based on form-factor approximation, or a modified form-factor approximation, or anomalous-scattering-factor corrections obtained through dispersion relations and photoeffect cross sections. For inelastic (Compton) scattering from bound electrons, impulse approximation has been used to obtain the Compton peak in the spectrum at given scattering angle, and the incoherent scattering factor has been used to give the total intensity of scattered radiation as a function of scattering angle.

For more detailed discussion of the S-matrix approach to Rayleigh scattering we call attention to the initial report of Kissel et al. (1980), the reviews of Kissel and Pratt (1985) and Kane et al. (1986), the corrected anomalous scattering factors of Kissel and Pratt (1990), the assessment of the validity of simpler approaches of Roy et al. (1983) and Zhou et al. (1992b), and works cited therein. The new S-matrix results for Compton scattering from inner-shell electrons were first reported by Suric et al. (1991) and a fuller discussion has now been presented by Bergstrom et al. (1992, 1993).

The reader should be alerted to differing sign conventions that are in common use in the literature. One convention involves the overall sign choice of the scattering amplitude. As the Thomson scattering amplitude is negative, some authors have explicitly factored out an overall minus sign (see, for example, James, 1965), while others have not (see, for example, Sakurai, 1967). A second important choice lies in the direction of propagation of a plane wave. The choice typically made in the physics literature, $exp\,(i\boldsymbol{K}\bullet\boldsymbol{r}-i\omega t)$, differs from that made in the crystallographic literature, $exp\,(i\boldsymbol{K}\bullet\boldsymbol{r}+i\omega t)$, with a consequent difference in the relative sign of the real and imaginary part of the scattering amplitude. We will not factor out the overall minus sign in our scattering amplitude A, and will use the plane wave convention of the physics literature. We will note the differences from the crystallographic literature in our final results for the anomalous scattering factors.

In section 2 of this paper we summarize some of general considerations which underlie the theoretical description of photon-atom scattering. We discuss the structure and partitioning of the scattering amplitudes and the dispersion relations and sum rules they satisfy. We discuss the scattering off a composite system as a scattering off bound charges, and the simple classical and quantum mechan-

ical descriptions of scattering off such systems of charges. We discuss the current state-of-the-art S-matrix approach and note its limitations. In section 3 we describe what has been achieved in Rayleigh scattering, the elastic scattering off bound electrons, and the extent of agreement with experiment. We review the simpler approaches to Rayleigh scattering and use the S-matrix results to assess their validity. We summarize the best current approach for the extensive presentation or tabulation of data, based on the use of modified form factors with relatively angle-independent anomalous scattering factors. In section 4 we summarize the new S-matrix results for Compton scattering, the inelastic scattering off bound electrons. In general the spectrum for scattering off inner-shell electrons has three structural features: the well-known Compton peak, resonant Raman Compton structure, and an even less well-known infrared rise. For elastic scattering we show comparisons with experiment. We discuss under what circumstances the usual impulse approximation provides an adequate description, for scattering off a given inner subshell and for scattering off the whole atom. In section 5 we review what has been learned about photon-atom scattering and give some outlook for further work.

2. MANY-BODY FORMALISM AND THE PARTITION OF SCATTERING AS SINGLE-PARTICLE TRANSITIONS

Elastic and inelastic scattering of photons are two of the main processes of photon-atom interaction. We can describe such processes in terms of a photon of momentum and polarization $(\boldsymbol{K}_i, \hat{\varepsilon}_i)$ incident on an atom and a photon of momentum and polarization $(\boldsymbol{K}_f, \hat{\varepsilon}_f)$ scattered from the atom. In elastic scattering the initial and final photon energies are the same, $|\boldsymbol{K}_i| = |\boldsymbol{K}_f|$. The interests in scattering from bound electrons of an atomic structure focus on the information we learn about the composite structure and its electron distribution. To set these scattering processes in context we show in Figures 1 and 2 their contributions to the total photon-absorption coefficient of representative atoms. Inelastic scattering is dominant for energies large compared to binding energies but below the pair production threshold; in these situations the absorption is fairly well understood as absorption from free electrons. Elastic scattering is only dominant for energies below all bound-electron thresholds. The intermediate region is dominated by photoelectric absorption, which however can lead to emission of de-excitation (e.g., fluorescence or relaxation) photons and so the same final state as in Compton scattering in the resonance region. Since photoeffect at these energies provides the dominant absorptive mechanism, it generally dominates the imaginary part of the elastic photon-atom scattering amplitude. Figures 1 and 2 differ from those used in the past in giving a more accurate rendition of low-energy elastic scattering from the S-matrix calculations, showing resonance behavior near photoelectric thresholds and a trend of decrease for low incident photon energies. At these energies the picture of inelastic scattering will also need to be modified.

Present state-of-the-art calculations of photon-atom scattering are based on numerical evaluations of the relativistic second-order S-matrix elements of external-field quantum electrodynamics within independent particle approximation

(IPA). That is, the atom is modeled as an infinitely massive nuclear charge and electrons moving in the common potential of that charge and an effective screening charge of all the electrons, without any direct interaction (correlations) among the electrons. Scattering in this model can therefore be described as elastic and inelastic scattering off the nucleus and the atomic electrons. In addition, since we are in a relativistic theory, there will be scattering off virtual pairs in the field (Delbrück scattering) or, in the language of hole theory, off the filled states of the negative-energy sea. (This is equivalent to allowing a sum over all intermediate states, filled or not.) In our discussion we will focus on scattering off the bound atomic electrons, but physically the processes are not entirely separable. In fact, in elastic scattering the initial and final states from scattering off the different components of the system cannot be distinguished, so that we must add their scattering amplitudes coherently. (In elastic scattering at x-ray energies, nuclear and Delbrück scattering contributions are small.) We shall see that care is also needed in applying the optical theorem and the dispersion relation connecting the real and the imaginary parts of the scattering amplitude.

Photon scattering from atoms is photon scattering from many-particle systems of electrons and nucleons which are held together by electromagnetic and nuclear forces. In addition to these particles, in the language of hole theory, the atomic system includes a filled negative-energy sea for each kind of particle. We shall not consider the forces (including those from radiation fields) which correlate motions of these particles, and so we will not have to deal with the pathologies of continuum dissolution (Brown-Ravenhall "disease", Brown and Ravenhall, 1951; Kim, 1993). This implies that the interactions among particles are treated at the independent particle approximation level, of which an example in atoms is the familiar central field approximation. It also implies that renormalization of particle states due to perturbations from external field quantum electrodynamics are not included

The interaction of radiation with this atomic system of particles and seas is described by introducing in the many-particle Hamiltonian the minimal electromagnetic coupling which for each particle of charge q replaces its momentum operator $\boldsymbol{p}$ by $\boldsymbol{p} - q\boldsymbol{A}/c$, with $\boldsymbol{A}$ the electromagnetic field at the coordinate of that particle. Then scattering of photons from this system of fermions (each satisfying a Dirac equation), to lowest non-vanishing order in perturbation theory, will be described by the second-order S-matrix amplitude

$$A = -\sum_P \left[\frac{\langle M | O_f^* | P \rangle \langle P | O_i | N \rangle}{E_N - E_P + \hbar\omega_i + i0_+} + \frac{\langle M | O_i | P \rangle \langle P | O_f^* | N \rangle}{E_N - E_P - \hbar\omega_f - i0_+} \right], \tag{1}$$

where $\hbar\omega_i$ ($\hbar\omega_f$) is the energy of the incident (scattered) photon, the operator O_i (O_f^*) describes the absorption (emission) of the incident (scattered) photon, $i = \sqrt{-1}$, and the states $|N\rangle$, $|M\rangle$ and $|P\rangle$ are solutions of the many-particle Dirac equation

$$H|I\rangle = E_I|I\rangle . \tag{2}$$

(In elastic scattering, the final state $|M\rangle$ is the same as the initial state $|N\rangle$, and $\hbar\omega_i = \hbar\omega_f$. In inelastic scattering, the final state $|M\rangle$ is excited, de-excited, or in the continuum.) The photon absorption and emission operators are expressed as

$$\begin{aligned} O_i &= \sum_j O_{ij} = \sum_j q_j \ \bar{\alpha} \bullet \hat{\varepsilon}_i \ e^{iK_i \bullet r_j} , \\ O_f^* &= \sum_j O_{fj}^* = \sum_j q_j \ \bar{\alpha} \bullet \hat{\varepsilon}_f^* \ e^{-iK_f \bullet r_j} , \end{aligned} \tag{3}$$

with $\boldsymbol{r}_j$ the position in the space of the jth particle. (We will write down some non-relativistic expressions subsequently. Here we are using relativistic expressions, so that in elastic scattering we can describe the partitioning of Rayleigh from Delbrück scattering.) The sum P in Eq. (1) is over a complete set of many-particle states for systems of the specified number of particles. Since the particles obey Fermi-Dirac statistics, in any given many-particle state only one particle is in a given state of the single-particle central potential. (Given that the set of particles includes filled negative-energy seas, both E_I and these sums are of course formal.)

It is traditional to partition the amplitude for scattering off an atomic system into amplitudes for scattering off its components - electrons, nucleons, the negative-energy seas - and in the case of elastic scattering (no energy transferred to the internal degrees of freedom of the atomic system) call these the component amplitudes for Rayleigh, Delbrück and nuclear Thomson scattering (to be added coherently, since they cannot be distinguished in any observation). Such a partition is not straight-forward. For example, one can see that for forward elastic scattering at very high energy off a bound system of two charges, the potential interaction between them may be neglected and one obtains scattering off two free charges. But in reality the scattering is to be described as from one free particle of the total mass and charge of the system and one particle of reduced mass and reduced charge in the presence of the potential interaction, yielding a very different scattering behavior at low energy (Kane et al., 1986). (In inelastic scattering we can define physical partitions in terms of initial single-particle states not observed in the final state; these will partition cross sections rather than matrix elements.)

Given the very different masses of electrons and nuclei, it is common in treating scattering at x-ray energies and below to take the nuclear mass as infinite. In this case there is no scattering from the nucleus, which serves only to absorb momentum (but not energy), and our scattering is only from the atomic electrons and the negative-energy electron sea. It is often supposed that (at higher energies) the changes due to finite nuclear mass are obtained by adding the amplitude for scattering off a free nucleus (nuclear Thomson scattering, nuclear resonance scattering etc.). Under this infinite nuclear mass assumption, the atomic system and the states of Eq. (1), which still applies, are described as states of electrons and an electron negative-energy sea. In the case of elastic scattering the states $|N\rangle$ and

$|M\rangle$ are now the same (no recoil of the system in scattering). And in this case of elastic scattering, we can write down for forward scattering $\boldsymbol{K}_i = \boldsymbol{K}_f$ without polarization change, $\hat{\varepsilon}_i = \hat{\varepsilon}_f$, the familiar optical theorem relating the imaginary part of the forward scattering amplitude without spin change to the total cross section (for absorption and scattering) for photons of the given polarization incident on the atomic system. We read out directly from Eq. (1)

$$\mathrm{Im}A(\omega, 0) = \frac{\omega}{4\pi c}\sigma^{\mathrm{TOT}} \approx \frac{\omega}{4\pi c}(\sigma^{\mathrm{PE}} + \sigma^{\mathrm{BBT+}} + \sigma^{\mathrm{PP}} + \sigma^{\mathrm{BPP}}) \tag{4}$$

where σ^{PE} is the cross section for photoeffect, $\sigma^{\mathrm{BBT+}}$ is the cross section for a transition from the initial state to a excited bound state of the system, σ^{PP} is the cross section for ordinary pair production with both the electron and positron created in the continuum, and σ^{BPP} is the cross section for bound pair production with the electron of the pair created in a bound state. In this order of our perturbation theory, we are relating the forward amplitude for elastic scattering (Rayleigh and Delbrück) to the total cross sections for photoeffect from the bound electrons of our atomic system and pair production in the field of our atomic system (including pair production with the electron produced in an unoccupied bound orbital).

It should be noted that our derivation of the optical theorem assumes that the state $|N\rangle$ from which we are scattering is the ground state of the system. If not, there are allowed intermediate states $|P\rangle$ of lower energy, and the second term of Eq. (1) will also contribute to the imaginary part of the amplitude, and the optical theorem (now in the presence of an energy source) becomes

$$\mathrm{Im}A(\omega, 0) = \frac{\omega}{4\pi c}\sigma^{\mathrm{TOT}} \approx \frac{\omega}{4\pi c}(\sigma^{\mathrm{PE}} + \sigma^{\mathrm{BBT+}} + \sigma^{\mathrm{PP}} + \sigma^{\mathrm{BPP}} - \sigma^{\mathrm{BBT-}} - \sigma^{\mathrm{BPA}}) \tag{5}$$

where $\sigma^{\mathrm{BBT-}}$ is the cross section for a transition from the initial state to a bound state of lower energy, and σ^{BPA} is the cross section for bound-electron pair annihilation wherein an initial hole in the negative-energy sea is filled by one of the initial bound electrons; we are to subtract a radiated flux associated with the filling of the vacancy (or, through detailed balance, with a cross section for absorbing a photon and creating a vacancy and an excited state). As there has been very little work thus far on scattering from excited states, this may seem an academic matter. But in fact, when we partition our elastic amplitude into Rayleigh and Delbrück components, each of them separately will have such a description, and the optical theorems for these partitioned components will include subtracted cross sections.

Since the interaction operator O is a sum of single-particle interaction operators, and the states are written as products of single-particle orbitals, it is possible to reduce the second-order amplitude, expressed in Eq. (1) in terms of transitions between many-particle states, to transitions between single-particle states. For elastic scattering we will thereby partition the amplitude into a sum of Rayleigh

and Delbrück amplitudes, the Rayleigh amplitude will be partitioned into a sum of amplitudes for scattering from each occupied bound-electron state, and we will obtain a corresponding partition of the optical theorem. But to do this will require a rearrangement and redefinition of the terms, in order that we work with sums over intermediate single-particle states which form complete sets. Related procedures must be applied for inelastic (Compton) scattering.

Inserting Eq. (3) for O into Eq. (1), in the case of elastic scattering we obtain

$$A = \sum_{n}^{\text{occ.}} \sum_{p}^{\text{uno.}} A_{np} = -r_0 mc^2 \sum_{n}^{\text{occ.}} \sum_{p}^{\text{uno.}} \left[\frac{\langle n| \mathcal{A}_f^* |p\rangle\langle p| \mathcal{A}_i |n\rangle}{E_n - E_p + \hbar\omega_i + i0_+} + \frac{\langle n| \mathcal{A}_i |p\rangle\langle p| \mathcal{A}_f^* |n\rangle}{E_n - E_p - \hbar\omega_f - i0_+} \right] , \quad (6)$$

where the sum is over occupied single-particle states $|n\rangle$ and unoccupied single-particle states $|p\rangle$, and $r_0 = e^2/mc^2 \approx 2.82 \times 10^{-15}$m is the classical electron radius. The electron states are solutions of the single-particle Dirac equation

$$H|i\rangle = E_i |i\rangle ,$$
$$H = c\bar{\alpha} \bullet \boldsymbol{p} + \beta c^2 + V(r) , \quad (7)$$

where $V(r)$ is the common central potential. The interactions with the initial and final photon wavefunctions are

$$\mathcal{A}_i = \bar{\alpha} \bullet \hat{\varepsilon}_i \; e^{iK_i \bullet r} ,$$
$$\mathcal{A}_f^* = \bar{\alpha} \bullet \hat{\varepsilon}_f^* \; e^{-iK_f \bullet r} . \quad (8)$$

Note that, to whatever intermediate single-particle state $|p\rangle$ the single-particle transition operator induced a transition from the single-particle state $|n\rangle$, we must have the same single-particle transition back in order to return the same initial many-particle state that we started from, justifying the single-particle transition form of Eq. (3). (This would not be true for the Compton matrix element.) Note that $A_{np} = -A_{pn}$. The sum n is over all occupied states of the atomic system, i.e. the bound atomic electron orbitals and the negative-energy sea. The sum p is over all unoccupied states of the system, i.e. the excited bound orbitals and the continuum. Thus in this form we would not be able to derive an optical theorem for the sum of amplitudes corresponding to scattering from a given atomic orbital $|n\rangle$, since the sum over intermediate states $|p\rangle$ is not complete. But given the antisymmetry of A_{np} we have

$$\sum_{n}^{\text{occ.}} \sum_{p}^{\text{occ.}} A_{np} = 0 , \quad (9)$$

and hence

$$A = \sum_{n}^{\text{occ.}} \sum_{p}^{\text{all}} A_{np} = -r_0 mc^2 \sum_{n}^{\text{occ.}} \sum_{p}^{\text{all}} \left[\frac{\langle n| \mathcal{A}_f^* |p\rangle\langle p| \mathcal{A}_i |n\rangle}{E_n - E_p + \hbar\omega_i + i0_+} + \frac{\langle n| \mathcal{A}_i |p\rangle\langle p| \mathcal{A}_f^* |n\rangle}{E_n - E_p - \hbar\omega_f - i0_+} \right] . \quad (10)$$

We may also partition A into Rayleigh and Delbrück amplitudes as

$$A = A^{\mathrm{R}} + A^{\mathrm{D}} , \quad (11)$$

where

$$A^{\mathrm{R}} = \sum_{n}^{\text{occ.}+} \sum_{p}^{\text{all}} A_{np} , \quad (12)$$

where the sum n is over all positive-energy occupied states, and

$$A^{\mathrm{D}} = \sum_{n}^{\text{occ.}-} \sum_{p}^{\text{all}} A_{np} , \quad (13)$$

where the sum n is over all negative-energy occupied states (the sea).

Note that we may now write optical theorems for each of these amplitudes separately. But we are now dealing with circumstances in which downward transitions are allowed. (This would cancel between A^{R} and A^{D}.) For the total Rayleigh scattering amplitude, summed over scattering from each atomic electron separately, the spurious resonances associated with bound-bound transitions between filled orbitals will cancel and need not be considered in writing an optical theorem for the total amplitude A^{R}. Real resonant transitions will remain associated with transitions to unoccupied states. However there will also be a subtracted cross section associated with downward transitions into real unoccupied bound states (this term survives the sum over occupied bound states only for scattering from excited states) and into the negative-energy states; the later can be identified with the cross section for positron annihilation with the electron of the given bound state. Thus the optical theorem for the imaginary part of the forward scattering amplitude from the bound atomic electrons will be

$$\mathrm{Im} A^{\mathrm{R}}(\omega, 0) = \frac{\omega}{4\pi c} (\sigma^{\mathrm{PE}} + \sigma^{\mathrm{BBT}+} - \sigma^{\mathrm{BBT}-} - \sigma^{\mathrm{BPA}}) \quad (14)$$

A similar discussion will apply to the Delbrück amplitude, in which, in addition to transitions from negative-energy electrons to the continuum (pair production cross section) we will have to add cross sections for transitions to the filled and unfilled bound states (bound pair production).

In the case of Compton scattering, inserting Eq. (3) for O into Eq. (1), we obtain analogous terms for achieving a single-particle transition from occupied orbital $|n\rangle$ to unoccupied orbital $|m\rangle$

$$A^{\mathrm{C1}} = -r_0 mc^2 \sum_p^{\mathrm{uno.}} \left[\frac{\langle m|\mathcal{A}_f^*|p\rangle\langle p|\mathcal{A}_i|n\rangle}{E_n - E_p + \hbar\omega_i + i0_+} + \frac{\langle m|\mathcal{A}_i|p\rangle\langle p|\mathcal{A}_f^*|n\rangle}{E_n - E_p - \hbar\omega_f - i0_+} \right]. \tag{15}$$

However now this is not the only way we can make such a single-particle transition, beginning with the many body matrix element of Eq. (1); there are additional terms not included in the sum above. Thus we can make single-particle transitions from occupied states $|p\rangle$ (and $|n\rangle$) to unoccupied states $|m\rangle$, and then, leaving $|m\rangle$ occupied, make a single-particle transition from $|n\rangle$ to $|p\rangle$. The corresponding single body transition matrix elements in this amplitude are

$$A^{\mathrm{C2}} = -r_0 mc^2 \sum_p^{\mathrm{occ.}} \left[\frac{\langle p|\mathcal{A}_f^*|n\rangle\langle m|\mathcal{A}_i|p\rangle}{E_p - E_m + \hbar\omega_i + i0_+} + \frac{\langle p|\mathcal{A}_i|n\rangle\langle m|\mathcal{A}_f^*|p\rangle}{E_p - E_m - \hbar\omega_f - i0_+} \right]. \tag{16}$$

Using the energy conservation relation

$$E_m = E_n + \hbar\omega_i - \hbar\omega_f, \tag{17}$$

and noting the over-all minus sign which came from the antisymmetry of the many body wave function, we see that these terms can be rearranged simply to represent the extension of the sum over intermediate states $|p\rangle$ in Eq. (15) to a sum over all intermediate states, empty and filled. Consequently, the amplitude for Compton scattering is

$$\begin{aligned} A^{\mathrm{C}} &= A^{\mathrm{C1}} + A^{\mathrm{C2}} \\ &= -r_0 mc^2 \sum_p^{\mathrm{all}} \left[\frac{\langle m|\mathcal{A}_f^*|p\rangle\langle p|\mathcal{A}_i|n\rangle}{E_n - E_p + \hbar\omega_i + i0_+} + \frac{\langle m|\mathcal{A}_i|p\rangle\langle p|\mathcal{A}_f^*|n\rangle}{E_n - E_p - \hbar\omega_f - i0_+} \right]. \end{aligned} \tag{18}$$

This result was established by Gavrila and Tugulea (1975) at the time they discovered the so-called resonant Raman contributions in L-shell Compton scattering. Thus we see that in both Rayleigh and Compton scattering it is correct to use single electron transition second-order S-matrix elements, with a sum over a complete set of intermediate states, occupied and unoccupied.

In all the S-matrix work to date (except some nonrelativistic analytic point-Coulomb calculations) one has summed or averaged scattering over all magnetic states of a subshell, thereby not considering the magnetic scattering effects that are possible with a polarized or oriented target.

3. FORMALISM OF SCATTERING AS SINGLE-PARTICLE TRANSITIONS

The scattering of radiation by an electron can also be described in nonrelativistic quantum mechanics. An appropriate nonrelativistic Hamiltonian can be written as

$$H = H_0 + H_{\text{int}} , \tag{19}$$

where

$$H_0 = \frac{p^2}{2m} + V(r) \tag{20}$$

is the Hamiltonian describing the interaction of the electron with the static potential $V(r)$ and

$$H_{\text{int}} = \frac{e^2}{2mc^2} A^2 - \frac{e}{mc} \boldsymbol{p} \bullet \boldsymbol{A} \tag{21}$$

describes the interaction of the electron with the photon. The corresponding nonrelativistic scattering amplitude involves three kinds of terms, two as in Eq. (12) or Eq. (18) (but without negative-energy states) and an additional term corresponding to the A^2 term of the nonrelativistic interaction Hamiltonian. The nonrelativistic Kramers-Heisenberg-Waller (KHW) scattering amplitude (Kramers and Heisenberg, 1925; Waller and Hartree, 1929) is written as

$$\begin{aligned} A_{nm}^{\text{KHW}} &= -r_0 \langle m| (\bar{\varepsilon}_i \bullet \bar{\varepsilon}_f^*) e^{-i\boldsymbol{K}\bullet\boldsymbol{r}} |n\rangle \\ &\quad -r_0 mc^2 \sum_p \left[\frac{\langle m| (\bar{\varepsilon}_f^* \bullet \boldsymbol{p}) e^{-i\boldsymbol{K}_f\bullet\boldsymbol{r}} |p\rangle\langle p| (\bar{\varepsilon}_i \bullet \boldsymbol{p}) e^{i\boldsymbol{K}_i\bullet\boldsymbol{r}} |n\rangle}{E_n - E_p + \hbar\omega_i + i0_+} \right. \\ &\quad \left. + \frac{\langle m| (\bar{\varepsilon}_i \bullet \boldsymbol{p}) e^{i\boldsymbol{K}_i\bullet\boldsymbol{r}} |p\rangle\langle p| (\bar{\varepsilon}_f^* \bullet \boldsymbol{p}) e^{-i\boldsymbol{K}_f\bullet\boldsymbol{r}} |n\rangle}{E_n - E_p - \hbar\omega_f} \right] , \end{aligned} \tag{22}$$

where $\boldsymbol{K} = \boldsymbol{K}_i - \boldsymbol{K}_f$ is the moment transferred by the photon, and the other quantities are the nonrelativistic counterparts of the corresponding quantities in Eq. (12) or Eq. (18). The additional term provides the basis for many of the familiar simpler calculations of elastic and inelastic scattering, form-factor and impulse approximation, and the incoherent scattering factor.

Since the scattering matrix elements are linear in the (complex) polarization

vectors $(\hat{\varepsilon}_i, \hat{\varepsilon}_f^*)$ which satisfy

$$\hat{\varepsilon}_i \bullet \boldsymbol{K}_i = \hat{\varepsilon}_f \bullet \boldsymbol{K}_f = 0 ,$$

the scattering cross sections are linear in $(1, \xi_1, \xi_2, \xi_3)$ with

$$\xi_1 = \varepsilon_x^* \varepsilon_x - \varepsilon_y^* \varepsilon_y , \quad \xi_2 = \varepsilon_x \varepsilon_y^* + \varepsilon_x^* \varepsilon_y , \quad \xi_3 = i(\varepsilon_x \varepsilon_y^* - \varepsilon_x^* \varepsilon_y) ,$$

the real Stokes parameters, for both initial and final polarizations. Here coordinate systems (different for initial and final photons) have been chosen such that $\bar{\varepsilon} = \varepsilon_x \hat{x} + \varepsilon_y \hat{y}$ with

$$|\varepsilon_x|^2 + |\varepsilon_y|^2 = 1$$

and $(\hat{x}, \hat{y}, \boldsymbol{K}_{i/f})$ a complete orthonormal set of unit vectors. For a given photon

$$\xi_1^2 + \xi_2^2 + \xi_3^2 = 1 .$$

If $\xi_3 = 0$, we are dealing with a linearly polarized photon; if $\xi_1 = \xi_2 = 0$, we are dealing with a circularly polarized photon. The Stokes parameters characterizing a beam of photons of given momentum may be defined as an average over the Stokes parameters of individual photons. In this case

$$\left[\bar{\xi}_1^2 + \bar{\xi}_2^2 + \bar{\xi}_3^2\right]^{1/2} \leq 1$$

and measures the degree of polarization of the beam.

In calculation of the matrix element from Eq. (12) or Eq. (18), the usual procedure is not to perform the infinite sum over intermediate states directly. Instead, following Brown et al. (1955) and the polarizability calculation of Dalgarno and Lewis (1955), one calculates numerically the inhomogeneous wavefunctions

$$|n_+\rangle = mc^2 \int_p \frac{|p\rangle\langle p|\mathcal{A}|n\rangle}{E_n - E_p + \hbar\omega_i} , \quad \langle m_-| = mc^2 \int_p \frac{\langle m|\mathcal{A}|p\rangle\langle p|}{E_n - E_p - \hbar\omega_f} , \tag{23}$$

satisfying the inhomogeneous wave equation

$$(H - E_n - \hbar\omega_f)\,|n_+\rangle = -mc^2 \mathcal{A}|n\rangle , \quad \langle m_-|\,(H - E_n + \hbar\omega_i) = -mc^2 \langle m|\mathcal{A} , \tag{24}$$

and the first order expression for the matrix element in terms of those functions

$$A_{nm} = r_0 [\langle m| \mathcal{A}^* |n_+\rangle + \langle m_-| \mathcal{A}^* |n\rangle] \ . \tag{25}$$

The S-matrix Rayleigh scattering calculations of Brown and co-workers (Brown et al., 1955; Brenner et al., 1955; Brown and Mayers, 1956, 1957), Johnson and co-workers (Johnson and Feiock, 1968; Lin et al., 1975; Johnson and Cheng, 1976) and Kissel and Pratt (Kissel et al., 1980; Roy et al., 1983); Parker and Pratt, 1984; Kissel and Pratt, 1985; Kane et al., 1986; Roy et al., 1987; Smend et al., 1987; Zhou et al., 1990, 1992b) and the Compton scattering calculations of Whittingham (1971, 1981) and Suric and co-workers (Suric et al., 1991; Bergstrom et al., 1992, 1993) have all been performed in this way, while the Compton scattering calculations of Wittwer (1972) were performed by directly summing over intermediate states.

An important approach to the calculation of the amplitude $A(\omega, \theta)$ for elastic scattering, not requiring the assumption of IPA but in practice restricted to the case of forward scattering, utilizes the analyticity of the forward scattering amplitude which follows from causality, leading to the dispersion relations

$$\begin{aligned} \mathrm{Re}A(\omega, 0) &= \frac{2\omega^2}{\pi} \int_0^\infty \frac{\mathrm{Im}A(\omega', 0)}{\omega'(\omega'^2 - \omega^2)} d\omega' , \\ \mathrm{Im}A(\omega, 0) &= -\frac{2\omega}{\pi} \int_0^\infty \frac{\mathrm{Re}A(\omega', 0)}{\omega'^2 - \omega^2} d\omega' , \end{aligned} \tag{26}$$

so that

$$\mathrm{Re}A(\infty, 0) = -\frac{2}{\pi} \int_0^\infty \frac{\mathrm{Im}A(\omega', 0)}{\omega'} d\omega' , \quad \mathrm{Im}A(\infty, 0) = 0 \ . \tag{27}$$

In nonrelativistic dipole approximation $\mathrm{Re}A^{\mathrm{R}}(\infty, 0) = -Nr_0$, with N the number of bound electrons. This is precisely the Thomas-Reiche-Kuhn sum rule (Thomas, 1925; Kuhn, 1925; Reiche and Thomas, 1925), where for the $\mathrm{Im}A^{\mathrm{R}}$ we insert Eq. (14). (Note, the single-particle form of this sum rule requires the partition we have made between A^{R} and A^{D}.) There are, however, small relativistic corrections to $\mathrm{Re}A^{\mathrm{R}}(\omega, 0)$, now understood as the amplitude for scattering off the bound electrons partitioned from the amplitude for Delbrück scattering. Another form of the dispersion relation may be written in terms of the real and imaginary parts g' and g'' of the anomalous amplitude referenced to the relativistic high-energy limit. These real quantities are defined by

$$A^{\mathrm{R}}(\omega, 0) - A^{\mathrm{R}}(\infty, 0) = -r_0 [g' + ig''] \ . \tag{28}$$

These anomalous scattering factors are closely related to the anomalous scattering factors f' and f'' conventionally defined in reference to the nonrelativistic high-energy limit, $-Nr_0$, as

$$g' = f' + \left(N + \frac{\mathrm{Re}A^{\mathrm{R}}(\infty, 0)}{r_0}\right), \quad g'' = f'' \ . \tag{29}$$

The sign of our f'' differs from that commonly given in the crystallographic literature f''_{CL} (see, for example, Cromer and Liberman, 1970b; Henke et al., 1981; Creagh and McAuley, 1992) as

$$f''_{\mathrm{CL}} = -f'' \ . \tag{30}$$

As noted in the introduction, this difference has its origins in a sign choice for the plane wave. This issue has been discussed in the previous conference on anomalous scattering by Ramaseshan et al. (1975) who pointed out problems comparing neutron and x-ray scattering where differing phase conventions are used.

The anomalous scattering factors satisfy

$$g'(\omega) = \frac{2}{\pi} \int_0^\infty \frac{\omega' g''(\omega')}{\omega'^2 - \omega^2} d\omega' \ . \tag{31}$$

In the nonrelativistic case g' reduces to the corresponding f'; the difference between g' and f' leads to a small constant correction to f' at all energies from nonrelativistic predictions. One now utilizes the optical theorem

$$\mathrm{Im}A^{\mathrm{R}}(\omega, 0) = -r_0 g''(\omega) = -r_0 f''(\omega) = \frac{\omega}{4\pi c} \sigma^{\mathrm{TOT}} \ , \tag{32}$$

which follows from the unitarity of the S-matrix, relating the total cross section for photon-atom scattering (elastic and inelastic, including absorption) to the imaginary forward elastic scattering amplitude. In fact in the partitioned relativistic amplitude, ordinary pair production, related to Delbrück scattering, is omitted from the total cross section, and pair production with an electron captured in a bound state of the potential is subtracted (required for convergence of the integral over the relativistic photoeffect cross section at high energies). As we have already seen, the total cross section at x-ray energies is dominated by absorption, primarily atomic photoelectric effect, but also includes contributions from bound-bound transitions (see, for example, Wang and Pratt, 1983), and these contributions must be included if accurate results are to be obtained from the dispersion relation for low-energy scattering. Subject to these qualifications, it should be possible to use better calculations of absorption (i.e. beyond IPA) or experimental data, and thereby obtain better predictions for forward elastic scattering.

Presently, the relativistic anomalous scattering factors computed by Cromer and Liberman (Cromer and Liberman, 1970a,b, 1976, 1981; Cromer 1974, 1983) or by others generally following their method (Henke et al., 1981, 1982, 1992; Creagh and McAuley, 1992) have come to be the most commonly used theoretical data set in the x-ray regime. But increasing attention is being drawn to the details of this approach where deficiencies in high-energy-limit values have been identified (Parker and Pratt, 1984; Smith, 1987; Kissel and Pratt, 1990). Another area of concern involves the neglect of bound-bound transitions, which will be especially important for lighter-Z atoms. Other numerical problems are also being reported (see the accompanying article by Chantler).

Simpler approaches to the scattering of photons from bound electrons begin with the neglect of electron binding and consider the scattering of photons from free electrons. The classical scattering of a photon from a free point charge is called Thomson scattering. The scattering amplitudes for incident photons linearly polarized parallel or perpendicular to the scattering plane are

$$A^{\mathrm{T}}_{||} = -r_0 \cos\theta \,, \quad A^{\mathrm{T}}_{\perp} = -r_0 \,, \tag{33}$$

leading to unpolarized differential and total cross sections

$$\frac{d\sigma^{\mathrm{T}}}{d\Omega} = \frac{r_0^2}{2}(1+\cos^2\theta) \,, \quad \sigma^{\mathrm{T}} = \frac{8}{3}\pi r_0^2 \,. \tag{34}$$

The same classical result is obtained for the total scattering cross section from a single extended particle of charge e described by an extended spherically symmetric charge distribution. However not all the scattering is coherent, corresponding to coherent scattering from different portions of the distribution. The coherent portion is obtained by multiplying the Thompson amplitudes by the real form factor

$$f(q) = 4\pi \int_0^\infty \rho(r) \frac{\sin(qr)}{qr} r^2 dr \,, \tag{35}$$

where $\rho(r)$ would describe the distribution of the charge normalized such that

$$4\pi \int_0^\infty \rho(r) r^2 dr = 1 \,. \tag{36}$$

Tabulations of the form factor based on nonrelativistic wavefunctions (Hubbell et al., 1975) and relativistic wavefunctions (Hubbell and Øverbø, 1979) are available.

The remainder of the amplitude would be understood as incoherent, corresponding to inelastic scattering. In Eq (35) we understand

$$\hbar q = |\boldsymbol{K}| = K = \frac{2\hbar\omega}{c}\sin\frac{\theta}{2} \tag{37}$$

as the momentum transferred by the scattered photon. This momentum transfer should be small in comparison to mc if we are to suppose the electron has not significantly been set into motion. That is, the Compton relation (Compton, 1923a,b

$$\hbar\omega_f = \frac{\hbar\omega_i}{1 + \frac{\hbar\omega_i}{mc^2}(1 - \cos\theta)} \tag{38}$$

for scattering of a photon (considered as a particle) off a free electron would correspond to inelastic scattering if the momentum transfer is not small.

Next we may consider the scattering off a collection of such extended particles. If the scattering is to be coherent, the individual amplitudes are to be added coherently, leading again to Eq (35), but with $\rho(r)$ now the total charge distribution of the system of particles, normalized here to Z rather than 1. The momentum transfer is to the system of particles, i.e. to the atom.

The same conclusions are obtained within quantum mechanics, assuming photon energies large compared to small binding energies and momentum transfers small compared to mc. In non-relativistic quantum mechanics these approximations are obtained from the A^2 term of the interaction Hamiltonian. If electron binding energies are not small in comparison to mc^2 there are additional relativistic binding effects which persist in the high-energy limit. For elastic scattering, Franz (1936) took these effects into account by replacing, for each electron, the form factor of Eq (35) by the modified form factor

$$g(q) = 4\pi \int_0^\infty \rho(r) \frac{\sin(qr)}{qr} \left[\frac{mc^2}{E - V(r)}\right] r^2 dr\,, \tag{39}$$

where E is the total energy (including rest mass energy) of the bound electron and $V(r)$ is the common central potential in which all electrons move. The modification may be traced to the propagator of the intermediate electron state; a similar modification may be applied in inelastic scattering. A tabulation of the resulting relativistic modified form factor for the whole atom has been given by Schaupp et al. (1983).

4. ELASTIC SCATTERING

The new S-matrix calculations for elastic scattering were first performed for scattering at γ-ray energies. Discrepancies between experiment and previous theory (Brown and Mayers, 1957) at 1.33 MeV were removed (Kissel et al., 1980).

Contributions to the total scattering amplitude attributed to Delbrück scattering could be identified in the experiments of Basavaraju et al. (1979) and Mückenheim and Schumacher (1980). Predictions for the γ-ray regime have been tabulated by Kane et al. (1986) for a variety of elements, energies, and scattering angles. A more comprehensive tabulation in this regime is feasible, utilizing interpolation methods.

Recently more attention has been focused on calculations of scattering at x-ray energies, including tracing through the regions of substantial anomalous scattering near edges. In Figure 4 we show an example of the comparisons of such calculations, and also simpler theories, of the differential cross section for scattering of 59.54 keV photons from Ta with the experiments of Schumacher and Stoffregen (1977) and of Govinda Nayak et al. (1992). Good agreement is achieved between experiment and the S-matrix calculation, while form-factor theories are not adequate unless anomalous scattering factors are included. In Figure 5 we show a comparison of calculations of the anomalous scattering factor f' for Ge with the experiments of Stanglmeier et al. (1992). Moderate, but not complete, agreement is achieved. The importance of the correct relativistic high-energy-limit expressions for f' is shown for Si in Figure 6. Agreement is achieved with the experiment of Deutsch and Hart (1988), clearly distinguished from an earlier result for the high-energy limit.

However with finer energy resolution, as can now be achieved with synchrotron radiation (SR) from the new storage rings, these IPA calculations will no longer be adequate near edges and resonances (even their positions are not correctly calculated), also for very soft photons. It is a challenge to perform better calculations, or even to design an adequate procedure for taking into account experimental information on edge and resonance positions.

It is also a challenge to identify simpler methods, not requiring the extensive computer time of the S-matrix approach, which can be used to provide needed extensive data sets in element, energy and angle. Zhou et al. (1992b) have compared predictions of the S-matrix calculation with predictions in the same potential of simpler approximations, such as form-factor and modified form-factor approximations. The next step in such approximations is to include anomalous scattering factors, taking g'' from photoeffect cross sections cut off at high energy by subtracting the corresponding bound pair production component, perhaps also including the bound-bound transition rates, and applying the dispersion relation and optical theorem to obtain g'. For forward scattering this will be identical with the S-matrix prediction in the same potential. It is found to be a fairly good approximation at x-ray energies to combine relativistic modified form factors with assumed angle-independent anomalous scattering factors to give predictions at finite scattering angle. (It would be a bad approximation to give anomalous scattering factors the same angle dependence as the form factor. Nevertheless complete angle independence is also not quite right. It appears that when these terms matter one can do better by assuming the whole anomalous factor has the angular dependence of the K shell, and that factor is represented by its nonrelativistic form in the point Coulomb potential, which is fairly simple.)

We illustrate in Figures 7 and 8 how well these various approximations reproduce the S-matrix results for representative elements. At high energy, form-factor

results are good in light elements, while anomalous factors matter in heavy elements. At low energies, form-factor results become constant, while anomalous terms result in decreasing cross sections. In light elements, the role of the bound-bound transitions in the dispersion integral is visible. And, of course, anomalous terms are essential in reproducing the "anomalous" behavior of the threshold regions. In light elements, modified form factors with angle-independent anomalous scattering factors well represent the S-matrix results while, for higher Z, as shown in Figure 9, there are deviations at higher energies for larger scattering angles that reflect the need to give some angular dependence to the anomalous amplitudes.

Let us summarize then the modified form factor with angle-independent anomalous-scattering-factor prescription (MF+ASF) we presently recommend as a relatively simple, relatively accurate scheme for estimating elastic scattering amplitudes and cross sections. General considerations of rotational invariance and parity conservation allow the elastic scattering amplitude to be written in the form

$$A^R = (\bar{\varepsilon}_i \bullet \bar{\varepsilon}_f^*)\ \mathcal{N}(\boldsymbol{K}_i \bullet \boldsymbol{K}_f) + (\bar{\varepsilon}_i \bullet \boldsymbol{K}_f)\ (\bar{\varepsilon}_f^* \bullet \boldsymbol{K}_i)\ \mathcal{M}(\boldsymbol{K}_i \bullet \boldsymbol{K}_f) \quad , \tag{40}$$

where $\mathcal{N}$ and $\mathcal{M}$ are complex functions of the scattering angle. Note only the first term contributes for forward scattering or in dipole or form-factor approximations; the second term is in general small through the x-ray regime and we will omit it in this scheme. Then we write the Rayleigh amplitude as

$$\mathcal{N}(\omega, \theta) = -r_0\,[g(q) + g'(\omega, \theta) + ig''(\omega, \theta)] \quad , \tag{41}$$

where under the assumption of angle-independent anomalous factors the reduced amplitude is written as

$$\mathcal{N}(\omega, \theta) = -r_0\,[g(q) + g'(\omega) + ig''(\omega)] \quad , \tag{42}$$

in terms of anomalous factors which vanish at high energy, related to the usual anomalous factors as

$$f'(\omega) = g'(\omega) + [g(q{=}0) - N] \quad , \quad f''(\omega) = g''(\omega) \quad . \tag{43}$$

One obtains g' in terms of g'' from the dispersion relation, Eq (31), and g'' from the optical theorem, Eq (32), in terms of the cross sections for photoeffect and bound pair production and the oscillator strengths for transitions between occupied bound states n and unoccupied bound states m. A complete consistent set of information (experimental or theoretical) on these processes can be used to obtain predictions for the elastic scattering amplitudes. (Recall that our sign convention for f'' differs from that customarily found in the crystallographic literature. See Eq. (30) and our earlier discussion.)

With the advent of SR it is of increased interest to discuss the photon polarization properties of the elastic scattering amplitude. The general formalism has

been given by Kane et al. (1986) and Roy et al. (1987); the latter paper discusses experiments in the γ-ray regime. Contrary to the simple form-factor predictions, polarization properties in general depend on atomic number and energy. In the x-ray regime, as we have indicated, the polarization properties may often be approximated as in Eq (41).

We may expect that correlation effects beyond IPA will have to be included in consideration of the anomalous-scattering region very near edges and the behavior of cross sections at very low energy. These effects shift edge positions and introduce further resonances. Only a few studies of such effects are available. We show in Figures (10) and (11) results of Zhou et al. (1992a) for Ar 3s photoeffect cross sections without and with correlations and the corresponding results for the 3s contribution to g' obtained via the optical theorem and dispersion relations. The effects of correlations are substantial. However, since elastic scattering is coherent, in this case the contributions from other subshells can substantially mask the features in a given subshell.

5. INELASTIC SCATTERING

Results from the new S-matrix code (Suric et al., 1991; Bergstrom et al., 1992, 1993) for the calculation of Compton scattering from bound electrons are becoming available. Thus far, attention has largely focused on the energy spectrum for scattering from a given inner subshell at given scattering angle. (Polarization dependence, whole-atom spectra, and cross sections at given scattering angle integrated over final energies have also been considered.) The three main possible structural features of these spectra are illustrated in Figure (12), showing in this case the infrared divergence which is always present in the limit of soft final-photon energies, resonances (resonant Raman scattering) related to downward transitions into lower occupied levels, and a Compton peak related to the energy-shifted line in scattering from a free electron (Compton, 1923a,b). The latter features can be (partially) hidden when the kinematic constraints on final energies are considered; the infrared divergence can sometimes affect such a small region of the spectrum that it is not seen within detector resolution or choices of sensitivity. These three features can be identified with the three terms of the nonrelativistic matrix element, Eq (22), and it is convenient to discuss them in this context, even though in fact the actual calculations are relativistic and relativistic modifications can be identified. Figure (12), like those which follow, in addition to the results of our numerical calculation also shows the results of various simpler approximations which we will discuss (Gavrila, 1969, 1972a,b, 1974; Costescu and Gavrila, 1973; Gavrila and Tugulea, 1975; Ribberfors, 1975a,b).

The Compton peak is first understood in terms of the scattering of a photon off a free electron, giving the line of the Compton relation, Eq (38), and then the broadening of that line which results if the initial free electron at rest is replaced by a momentum distribution of free electrons corresponding to the momentum distribution associated with the bound electrons. This is illustrated in Figure (13). The peak is obtained in evaluation of the nonrelativistic A^2 interaction term of the Hamiltonian, as in the early work of Schnaidt (1934) using point-Coulomb wave

functions and much subsequent work. Most commonly, however, the final ejected electron is represented as a plane wave, leading to the impulse-approximation representation of the spectrum in terms of the Compton profile (see, for example, Biggs et al., 1975)

$$\frac{d^2\sigma}{d\omega_f d\Omega_f} = \alpha^2 \left(\frac{1+\cos^2\theta}{2}\right) \frac{\omega_f}{\omega_i}\frac{1}{K} J_{nl}(p_z) \ , \tag{44}$$

where the Compton profile is

$$J_{nl}(p_z) = \frac{1}{2}\int_{p_z}^{\infty} \frac{I_{nl}(p)}{p} dp \ , \tag{45}$$

with

$$I_{nl} = |\chi_{nl}(p)|^2 p^2 \tag{46}$$

in terms of the Fourier transform χ_{nl} of the wave function of the scattering state, and the projection of bound-electron momentum on the direction of photon momentum transfer is

$$p_z = \frac{E(\hbar\omega_i - \hbar\omega_f) - \hbar\omega_i \hbar\omega_f (1-\cos\theta)}{c^2 K} \ . \tag{47}$$

Relativistic versions of impulse approximation have also been used (Eisenberger and Reed, 1974; Manninen et al., 1974; Ribberfors, 1975a,b). It has usually been supposed that the impulse approximation is valid when the photon momentum transfer is much bigger than the expectation value of bound-electron momentum. Suric (1992) has recently proposed a more sensitive criterion which appears to be in accord with the numerical calculations. It should be noted that Eq (44), as often used (see, for example, Biggs et al., 1975), does not recognize that there is a kinematic limit on final photon energy associated with the binding energy of the electron; this can cut the spectrum before the peak. (Usually in total-atom scattering, where the peak is dominated by scattering from outer-shell electrons, this is not a problem, as the small outer-shell binding energy does not exclude the peak energy.) Examples of spectra dominated by the Compton peak are shown in Figures (14-16). Figure (14) illustrates a situation in which relativistic effects are very important; relativistic impulse approximation (Ribberfors, 1975a,b) does quite well in reproducing the peak region of the spectrum. In Figure (15) for a lighter atom nonrelativistic impulse approximation is adequate. More of the upper side of the peak is cut off by the kinematic limit, and the soft-photon infrared rise is visible in somewhat more of the spectrum. Figure (16) shows a lighter element at lower energy and back angles. The peak is now kinematically forbidden and all one sees is the rise on the lower side of the peak. The soft-photon infrared rise occupies

nearly half the spectrum.

We may expect on general grounds (low-energy theorem - Low, 1958; Burnet and Kroll, 1968; Jauch and Rohrlich, 1976) that there must be an infrared rise for emission of soft scattered photons and that in this case the matrix element for Compton scattering (soft final photon) must be proportional to that for photoeffect (no final photon). In this region the doubly differential cross section for Compton scattering may be written in terms of the photoeffect angular distribution $d\sigma^{pe}/d\Omega_f$ as

$$\frac{d^2\sigma}{d\omega_f d\Omega_f} = \frac{\alpha}{(2\pi)^2 c}\frac{v_2^2}{\omega_f}\int \frac{\left[1-(\hat{p}_2\bullet\hat{k}_f)^2\right]}{\left[1-v_2(\hat{p}_2\bullet\hat{k}_f)^2\right]}\frac{d\sigma^{pe}}{d\Omega_2}d\Omega_2 , \tag{48}$$

where the integral is over the angles Ω_2 of photoelectron emission (v_2 is the velocity and $\hat{p}_2$ is emission direction of the photoelectron). The infrared rise is associated with the absorption-first matrix element. It was exhibited explicitly in the nonrelativistic Coulomb dipole calculations of Gavrila (1969, 1972a,b, 1974). Efforts to observe it experimentally have not yet been successful (Marchetti and Franck, 1987, 1989, 1990; Basavaraju et al., 1987; Briand et al., 1989, 1990; Lad et al., 1990; Simionvici et al., 1990). Since it is proportional to the photoeffect cross section, we can anticipate that in whole-atom scattering it is dominated by the innermost shell that is kinematically allowed. We have already seen illustrations of the effect in the previous figures. We note that in many cases Gavrila's expression is quite good, reflecting the fact that inner-shell photoeffect total cross sections can be well represented by nonrelativistic dipole point-Coulomb cross sections. Further results of these kinds are shown in Figures (17) and (18). Note in the latter case that the spectrum is almost completely dominated by the soft-photon behavior, well-predicted by the low-energy theorem, and shows only a vestige of the Compton peak rise. At back angles there are large differences from Gavrila's expressions.

The emission-first matrix element exhibits resonances, as was exhibited explicitly in calculations of Costescu and Gavrila (1973) and Gavrila and Tugulea (1975) for the L shell. When the emitted photon energy is near the transition energy, the resonance dominates the spectrum, as was observed by Sparks (1974). Evidently resonances will occur in scattering from a given subshell whenever there is an allowed transition to a lower subshell in the single-particle matrix element. We illustrate the phenomena in Figures (19, 20), contrasting L1 and L3 spectra at several incident energies going through the K edge. For the L1 spectrum there are no allowed dipole transitions. With increasing energy more of the Compton peak is kinematically allowed, though not yet its maximum. (Impulse approximation suggests a fine structure associated with the nodal structure of the wave function, which occurs only on the high-energy side of the peak in more exact calculations where it is kinematically allowed.) The infrared rise region is still significant even at the highest energy. Many of these features are still present in the L3 spectrum, though the infrared rise is less significant at the higher energies corresponding to a more rapidly decreasing photoeffect cross section. But there is the

additional resonance term. For an incident energy well below the K edge it has only a slight influence on the cross section. For an incident energy just below the K edge, the whole spectrum is resonance dominated; the cross section for hard final photons is very much larger, often by orders of magnitude, than impulse approximation would predict. For an incident energy well above the K edge the hard-photon region of the spectrum is approaching impulse approximation (the peak is not yet kinematically allowed). The resonance is still present, but has shifted to the middle of the spectrum. In considering Compton scattering from higher shells there can be a series of resonances in the same spectrum, corresponding to fluorescence transitions in these outer shells.

If we consider Compton scattering from the whole atom, summed over subshells (as in experiments not detecting the ejected electron or the transition radiation filling the vacancy), the Compton peak region is dominated by scattering from outer (loosely bound) electrons and is generally well described in impulse approximation. The soft-photon infrared rise will be dominated by the innermost kinematically allowed shell (Bergstrom et al., 1992). In between there will be a series of resonant peaks; in some cases these will be superimposed on the other features.

Often one asks for the total cross section for scattering photons (of any energy) into a given angle; in impulse approximation this is described by the incoherent scattering factor. One also integrates then over angle to get a total cross section, a component of the total absorption coefficient. In view of our discussion of the infrared divergence of the spectrum it is clear that quantities so described do not exist. The solution to this problem lies in realizing that one must also consider the radiative corrections to photoeffect (McEnnan and Gavrila, 1977; Botto and Gavrila, 1982), which include that part of Compton scattering below a specified level of resolution (i.e. the infrared region). With any specified resolution the cross sections for both processes are finite. And the sum of the cross sections, as in the absorption coefficient, is independent of the resolution chosen. Numerical calculations suggest that through the x-ray and soft γ-ray regimes the traditional practice of calculating photoeffect neglecting radiative corrections and Compton scattering in impulse approximation is adequate (Bergstrom, 1992).

6. CONCLUSIONS

We have seen that, with S-matrix methods, considerable progress has been made in providing a more detailed understanding of photon-atom scattering processes and assessing the validity of simpler approaches. One can envisage the possibility of more systematic tabulation of cross sections, efficient and faster codes for calculation, and simple prescription schemes for estimates. Agreement with experiment is encouraging, but not complete.

First principle calculations, particularly near edges, will require the inclusion of electron correlation effects; a satisfactory alternative scheme incorporating experimental information (such as edge positions) would be desirable. There are fundamental issues still to resolve in the partitioning of the scattering matrix element and the consequent partitioning of dispersion relations. Dependence of cross sections on polarization and of anomalous factors on angle, need to be worked

through. Magnetic scattering has not been addressed at this S-matrix level. Inelastic scattering calculations need to be extended to include coincidences with ejected electrons. Effects of the photon-atom scattering environment open many new issues. The atom may be in a molecule, plasma, surface or solid; the photon may be part of an intense beam in which many-photon interaction effects must be considered. There are thus many opportunities for further and interesting work in this field.

We wish to thank Tihomir Suric for the use of his computer codes. We thank all those who have participated with us in these studies, especially Bin Zhou, Suprakash Roy and Prabhakar Kane. This work has been supported in part by the U. S. National Science Foundation under grant PHY90-05763. It has also in part been performed under the auspices of the U. S. Department of Energy by Lawrence Livermore National Laboratory under contract number W-7405-ENG-48. Some of our calculations were performed under grant PHY89-0015P at the Pittsburgh Supercomputing Center (PSC). One of us (PMB) wishes to thank Michael Kopko of the PSC for his assistance.

7. REFERENCES

Basavaraju, G., P. P. Kane and K. M. Varier (1979) Pramana **12**, 665.

Basavaraju, G, P. P. Kane and S. M. George (1987) Phys. Rev. A **36**, 655.

Bergstrom, Jr., P. M. (1992) Ph. D. Thesis, Department of Physics and Astronomy, University of Pittsburgh, Pittsburgh, PA, USA.

Bergstrom, Jr., P. M., T. Suric, K. Pisk and R. H. Pratt (1992) Nucl. Instrum. Methods B **71**, 1.

Bergstrom, Jr., P. M., T. Suric, K. Pisk and R. H. Pratt (1993) Phys. Rev. A **48** (scheduled for August, 1993).

Biggs, F., L. B. Mendelsohn and J. B. Mann (1975) At. Data Nucl. Data Tables **16**, 201.

Botto, D. and M. Gavrila (1982) Phys. Rev. A **26**, 237.

Brenner, S., G. E. Brown and J. B. Woodward (1955) Proc. Roy. Soc. (Lond.) **A227**, 59.

Briand, J. P., A. Simionvici, P Chevallier and P. Indelicato (1989) Phys. Rev. Lett. **62**, 2092.

Briand, J. P., A. Simionvici, P Chevallier and P. Indelicato (1990) Phys. Rev. Lett. **65**, 269.

Brown, G. E. and D. F. Mayers (1956) Proc. Roy. Soc. (Lond.) **A233**, 527.

Brown, G. E. and D. F. Mayers (1957) Proc. Roy. Soc. (Lond.) **A242**, 89.

Brown, G. E., R. E. Peierls and J. B. Woodward (1955) Proc. Roy. Soc. (Lond.) **A227**, 51.

Brown, G. E. and D. G. Ravenhall (1951) Proc. Roy. Soc. (Lond.) **A208**, 552.

Burnet, T. H. and K. M. Kroll (1968) Phys. Rev. Lett. **20**, 86.

Compton, A. H. (1923a) Phys. Rev. **21**, 483.

Compton, A. H. (1923b) Phys. Rev. **22**, 409.

Creagh, D. C. and W. J. McAuley (1992) in *International Tables for Crystallography*, Vol. C, A. J. C. Wilson, ed. (Kluwer, Dordrecht) p. 206.

Costescu, A. and M Gavrila (1973) Rev. Roum. Phys. **18**, 493.
Cromer, D. T. (1974) in *International Tables for X-ray Crystallography*, Vol. IV, J. A. Ibers and W. C. Hamilton, ed. (Kynoch Press, Bermingham) pp. 148-150.
Cromer, D. T. (1983) J. Appl. Cryst. **16**, 437.
Cromer, D. T. and D. Liberman (1970a) Los Alamos Scientific Laboratory Report LA-4403, 163 pp., Los Alamos, NM, USA.
Cromer, D. T. and D. Liberman (1970b) J. Chem. Phys. **53**, 1891.
Cromer, D. T. and D. Liberman (1976) Acta Cryst. A **32**, 339.
Cromer, D. T. and D. Liberman (1981) Acta Cryst. A **37**, 267.
Dalgarno, A. and J. T. Lewis (1955) Proc. Roy. Soc. (Lond.) **A233**, 70.
Deutsch, M. and M. Hart (1988) Phys. Rev. B **37**, 2701.
Eisenberger, P. and W. A. Reed (1974) Phys. Rev. B **9**, 3237.
Franz, W. (1936) Z. Phys. **98**, 314.
Gavrila, M. (1969) Lett. Nuov. Cim. **5**, 180.
Gavrila, M. (1972a) Phys. Rev. A **6**, 1348.
Gavrila, M. (1972b) Phys. Rev. A **6**, 1360.
Gavrila, M. (1974) Rev. Roum. Phys. **19**, 473.
Gavrila, M. and M. N. Tugulea (1975) Rev. Roum. Phys. **20**, 209.
Henke, B. L., P. Lee, T. J. Tanaka, R. Shimabukuro and B. K. Fujikawa (1981) in *Low Energy X-ray Diagnostics - 1981 (Monterey)*, AIP Conf. Proc. No. 75, D. T. Attwood and B. L. Henke, ed. (American Institute of Physics, New York) pp. 340-388.
Henke, B. L., P. Lee, T. J. Tanaka, R. Shimabukuro and B. K. Fujikawa (1982) At. Data Nucl. Data Tables **27**, 1.
Henke, B. L., E. M. Gulliksen and J. C. Davis (1992) At. Data Nucl. Data Tables (in preparation).
Hubbell, J. H. and I. Øverbø (1979) J. Phys. Chem. Ref. Data **8**, 69.
Hubbell, J. H., W. J. Veigele, E. A. Briggs, R. T. Brown, D. T. Cromer and R. J. Howerton (1975) J. Phys. Chem. Ref. Data **4**, 471; erratum in (1977) J. Phys. Chem. Ref. Data **6**, 615.
Govinda Nayak, N., K. Siddappa, K. M. Balakrishna and N. Lingappa (1992) Phys. Rev. A **45**, 4490.
Jauch, M. and F. Rohrlich (1976) *The Theory of Photons and Electrons: The Relativistic Quantum Field Theory of Charged Particles with Spin One-Half* (Springer-Verlag, New York) 2nd ed.
James, R. W. (1965) *The Optical Principles of the Diffraction of X-Rays* (Cornell U. Press: Ithaca, New York).
Johnson, W. R. and F. D. Feiock (1968) Phys. Rev. **168**, 22.
Johnson, W. R. and K. T. Cheng (1976) Phys. Rev. A **13**, 692.
Kane, P. P., L. Kissel, R. H. Pratt and S. C. Roy (1986) Phys. Reports **140**, 75.
Kim, Y.-K. (1993) Comment At. & Molec. Phys. **28**, 201 (1993).
Kissel, L., R. H. Pratt and S. C. Roy (1980) Phys. Rev. A **22**, 1970.
Kissel, L. and R. H. Pratt (1985) "Rayleigh scattering: Elastic photon scattering by bound electrons," in *Atomic Inner-Shell Physics*, ed. B. Crasemann (Plenum Press, New York) ch. 11.
Kissel, L. and R. H. Pratt (1990) Acta Cryst. A **46**, 170.

Kramers, H. A. and W. Heisenberg (1925) Z. Phys. **31**, 681.
Kuhn, W. (1925) Z. Phys. **33**, 408.
Lad, S. M., G. Basavaraju and P. P. Kane (1990) Phys. Rev. A **42**, 1267.
Lin, C. P., K. T. Cheng and W. R. Johnson (1975) Phys. Rev. A **11**, 1946.
Low, F. E. (1958) Phys. Rev. 110, 974.
Manninen, S., T. Paakkari and K. Kajante (1974) Philos. Mag. **29**, 167.
Marchetti, V. and C. Franck (1987) Phys. Rev. Lett. **59**, 1557.
Marchetti, V. and C. Franck (1989) Phys. Rev. A **39**, 647.
Marchetti, V. and C. Franck (1990) Phys. Rev. Lett. **65**, 268.
McEnnan, J. and M. Gavrila (1977) Phys. Rev. A **15**, 1537.
Mückenheim, W. and M. Schumacher (1980) J. Phys. G **6**, 1237.
Parker, J. C. and R. H. Pratt (1984) Phys. Rev. A **29**, 152.
Ramaseshan, F., T. G. Ramesh and G. S. Ranganath (1975) in *Anomalous Scattering*, F. Ramaseshan and S. C. Abrahams, ed. (Munksgaard: Copenhagen) pp. 139-161.
Ribberfors, R. (1975a) Phys. Rev. B **12**, 2067.
Ribberfors, R. (1975b) Phys. Rev. B **12**, 3136.
Reiche, F. and W. Thomas (1925) Z. Phys. **34**, 510.
Roy, S. C., L. Kissel and R. H. Pratt (1983) Phys. Rev. A **27**, 285.
Roy, S. C., B. Sarkar, L. Kissel and R. H. Pratt (1987) Nucl. Instrum. Methods **A255**, 66.
Sakurai, J. J. (1967) *Advanced Quantum Mechanics* (Addison-Wesley: Reading, Massachusetts).
Schaupp, D., M. Schumacher, F. Smend, P. Rullhusen and J. H. Hubbell (1983) J. Phys. Chem. Ref. Data **12**, 467.
Schnaidt, F. (1934) Ann. Phys. (Leipz.) **21**, 89.
Schumacher, M. and A. Stoffregenn (1977) Z. Phys. A **283**, 15.
Simionvici, A., J. P. Briand, P. Indelicato and P. Chevallier (1990) Phys. Rev. A **41**, 3707.
Smend, F., D. Schaupp, H. Czerwinski, M. Schumacher, A. H. Millhouse and L. Kissel (1987) Phys. Rev. A **36**, 5189.
Smith, D. Y. (1987) Phys. Rev. A **35**, 3381.
Sparks, Jr., C. J. (1974) Phys. Rev. Lett. **33**, 262.
Stanglmeier, F., B. Lengeler, W. Weber, H. Göbel an M. Schuster (1992) Acta Cryst. A **48**, 626.
Suric, T. (1992) Nucl. Instrum. Methods A **314**, 240.
Suric, T., P. M. Bergstrom, Jr., K. Pisk and R. H. Pratt (1991) Phys. Rev. Lett. **67**, 189.
Thomas, W. (1925) Naturwiss. **13**, 627.
Waller, I. and D. R. Hartree (1929) Proc. Roy. Soc. (Lond.) **A124**, 119.
Wang, M. S. and R. H. Pratt (1983) Phys. Rev. A **28**, 3115.
Whittingham, I. B. (1971) J. Phys. A **4**, 21.
Whittingham, I. B. (1981) Aust. J. Phys. **34**, 163.
Wittwer, L. A. (1972) Lawrence Radiation Laboratory Report UCRL-51268, Livermore, CA, USA.
Zhou, B., R. H. Pratt, S. C. Roy and L. Kissel (1990) Phyica Scripta **41**, 495.

Zhou, B., L. Kissel and R. H. Pratt (1992a) Phys. Rev. A **45**, 6909.
Zhou, B., S. C. Roy, L. Kissel, S. K. Sen Gupta and R. H. Pratt (1993) in preparation.

Figure Captions

Figure 1. Integrated photon-atom cross sections for $_6$C: ELASTIC - Rayleigh scattering; INELASTIC - bound Compton scattering; PE - photoeffect; PP - pair production; TOTAL - sum of all cross sections.

Figure 2. Same as Figure 1 for $_{82}$Pb.

Figure 3. Furry diagrams of 2nd-order scattering.

Figure 4. Comparison of theory with experiment for 59.54 keV photons on $_{73}$Ta: SM - S matrix; NF - nonrelativistic form factor; RF - relativistic form factor; MF - modified form factor; MF+ASF - MF with angle-independent anomalous scattering factors; ● -Schumacher and Stoffregen (1977); □ - Govinda Nayak et al. (1992).

Figure 5. Comparison of theory with experiment for f' of $_{29}$Cu: ● - Stanglmeier et al. (1992).

Figure 6. Comparison of Cromer and Liberman (C+L – Cromer, 1983) f', with and without high-energy-limit correction (Kissel and Pratt, 1990), with experiment of Deutsch and Hart (1988) for $_{14}$Si.

Figure 7. Differential cross section for $_6$C from theory: SM (×) - S matrix; MF (– – –) - modified form factor; MF+ASF (solid curve) - MF with angle-independent anomalous scattering factors; MF+ASF-BB (- - -) - MF+ASF without bound-bound contributions.

Figure 8. Same as Figure 7 for $_{82}$Pb.

Figure 9. Relative error in MF+ASF predictions as compared with SM for $_{82}$Pb.

Figure 10. RRPA vs. HFSL predictions of photoeffect for the 3s subshell of $_{18}$Ar.

Figure 11. Same as Figure 10 for g'.

Figure 12. Main spectral features of Compton scattering as seen in the L_{II} subshell for $_{82}$Pb, 279 keV, $\theta = 135°$ (cross section is per electron). The following symbols are used for this and all subsequent figures, not all theories in each figure: × – S matrix; + – Wittwer (1972); ○ – point-Coulomb dipole $\boldsymbol{p} \bullet \boldsymbol{A}$ (Gavrila and co-workers); □ – low-energy theorem; (—·—·—) – relativistic impulse approximation; (– – –) – nonrelativistic A^2 (Schnaidt, 1934); (- - -) – impulse approximation (Biggs et al., 1975).

Figure 13. Sharp line of free-electron Compton scattering contrasted with shifted and broadened peak of bound-electron Compton scattering.

Figure 14. Same as Figure 12 for the K shell of $_{82}$Pb, 662 keV, $\theta = 135°$.

Figure 15. Same as Figure 12 for the K shell of $_{29}$Cu, 100 keV, $\theta = 135°$.

Figure 16. Same as Figure 12 for the K shell of $_{13}$Al, 17.4 keV, $\theta = 135°$.

Figure 17. Same as Figure 12 for the K shell of $_{6}$C, 2.94 keV, $\theta = 135°$.

Figure 18. Same as Figure 12 for the K shell of $_{79}$Au, 145 keV, $\theta = 150°$.

Figure 19. Same as Figure 12 for the L_I subshell of $_{28}$Ni, $\theta = 120°$.

Figure 20. Same as Figure 19 for the L_{III} subshell.

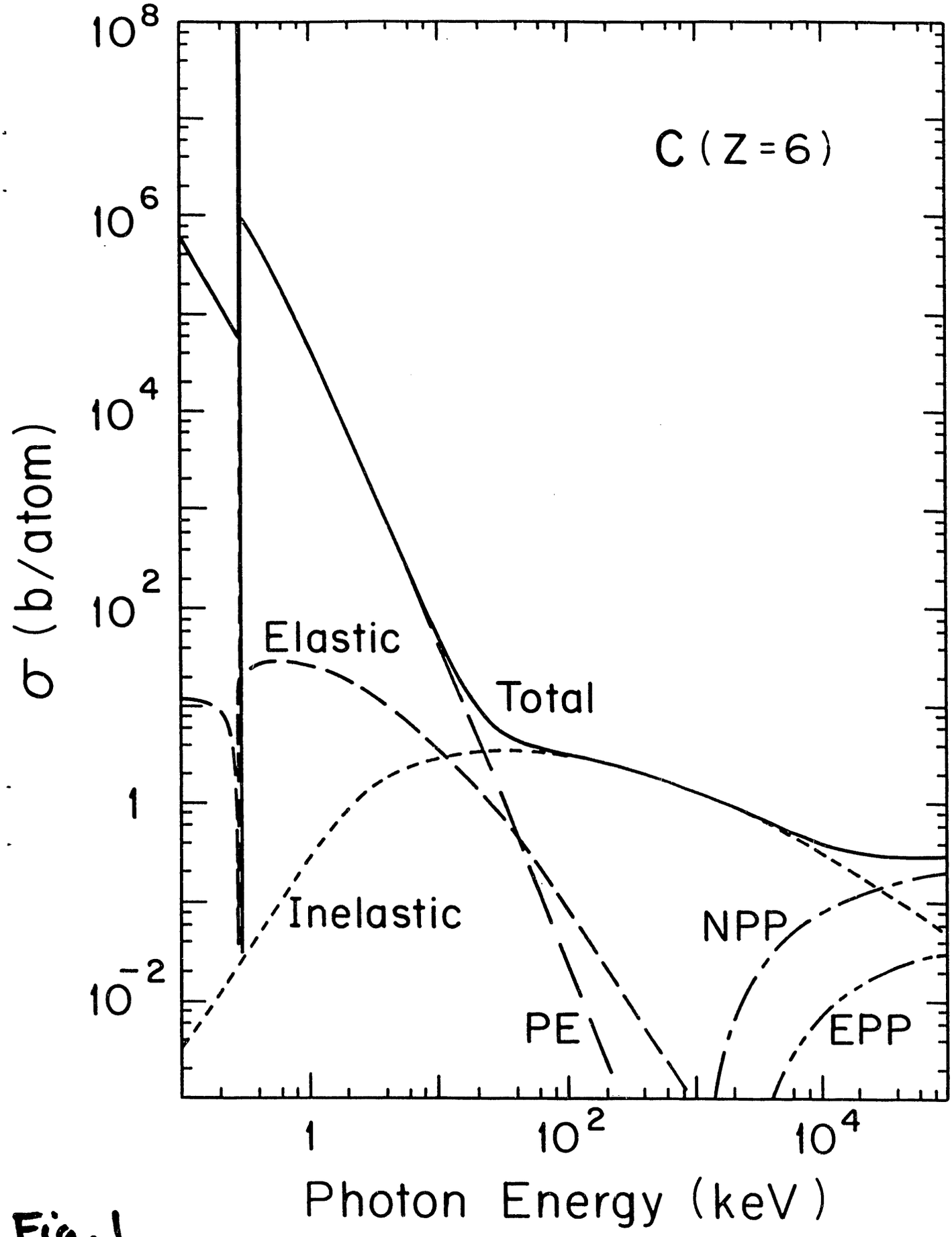
C (Z=6)
Elastic
Total
Inelastic
NPP
PE
EPP
σ (b/atom)
Photon Energy (keV)
10^8
10^6
10^4
10^2
1
10^{-2}
1
10^2
10^4

Fig. 1

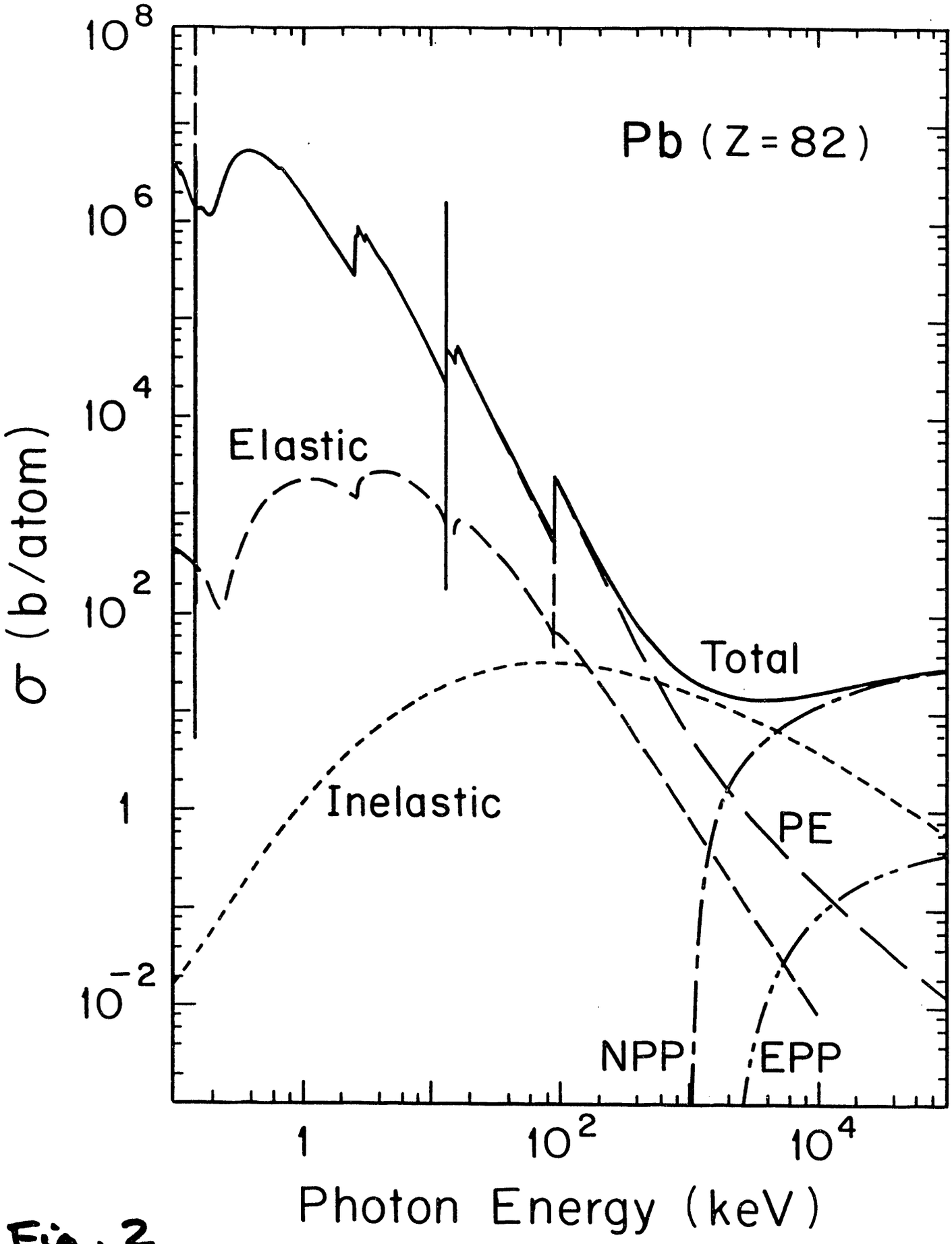
Pb (Z = 82)
Elastic
Inelastic
Total
PE
NPP
EPP
σ (b/atom)
Photon Energy (keV)
10^8
10^6
10^4
10^2
1
10^{-2}
1
10^2
10^4

Fig. 2

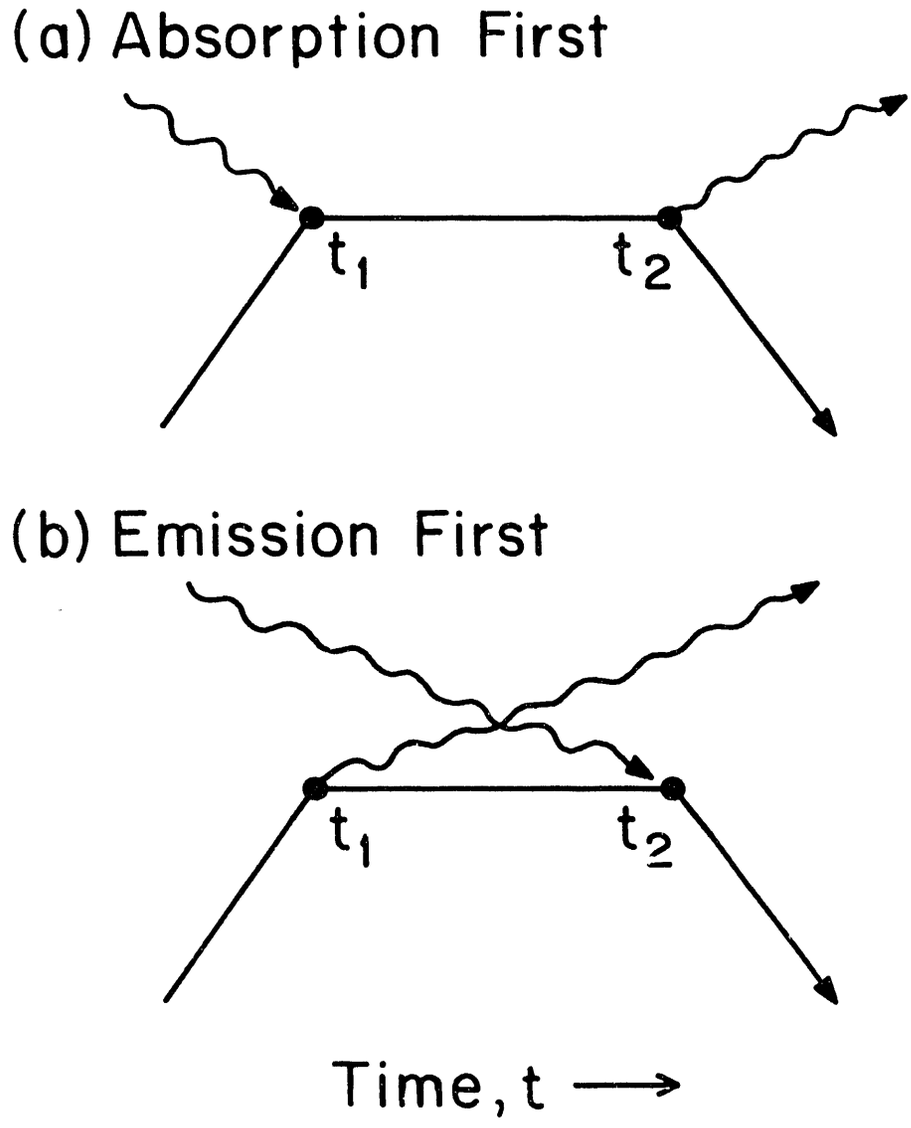

Fig. 3

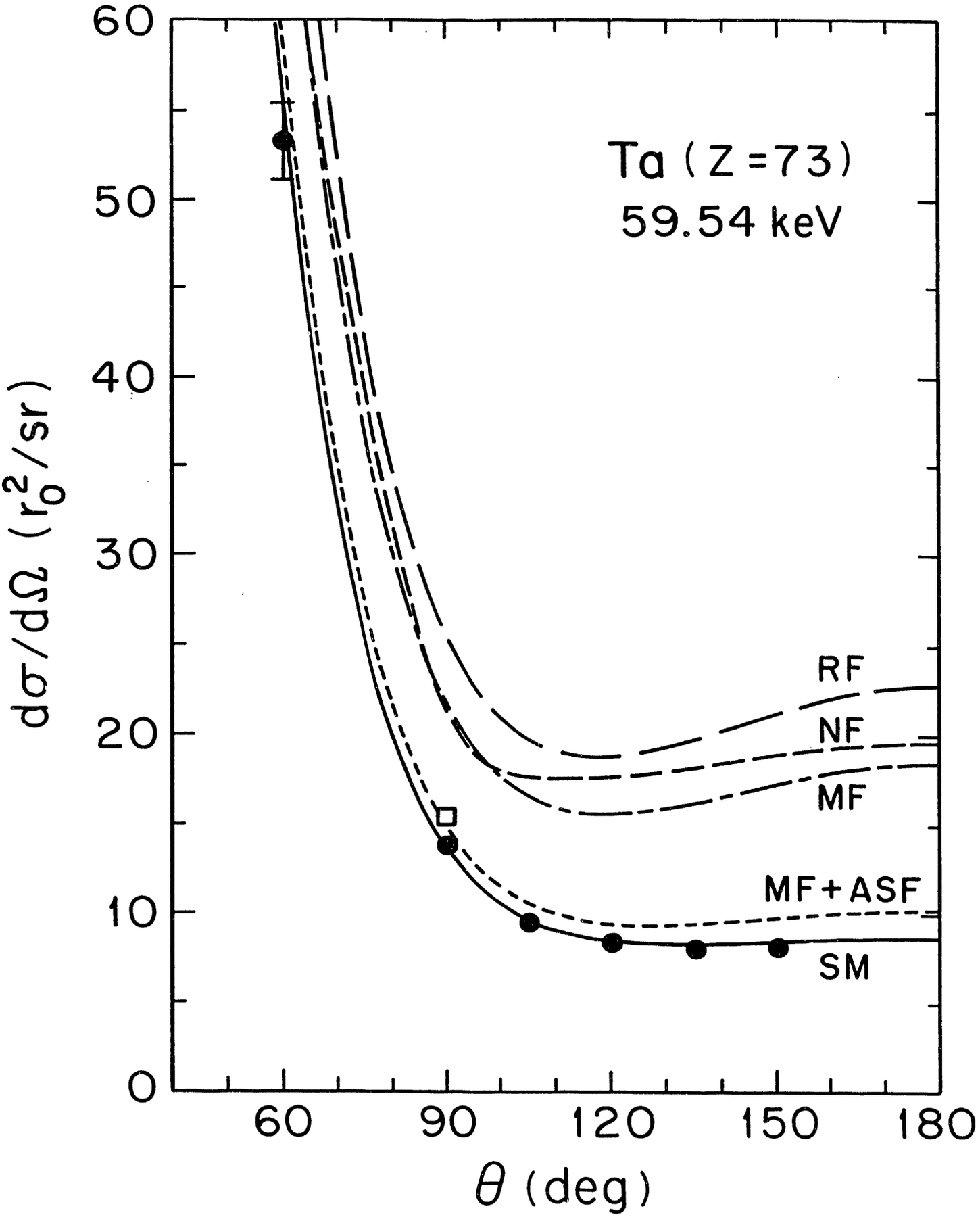
Ta (Z = 73)
59.54 keV
RF
NF
MF
MF + ASF
SM
$d\sigma/d\Omega$ (r_0^2/sr)
θ (deg)
0
10
20
30
40
50
60
60
90
120
150
180

Fig. 4

Fig. 5

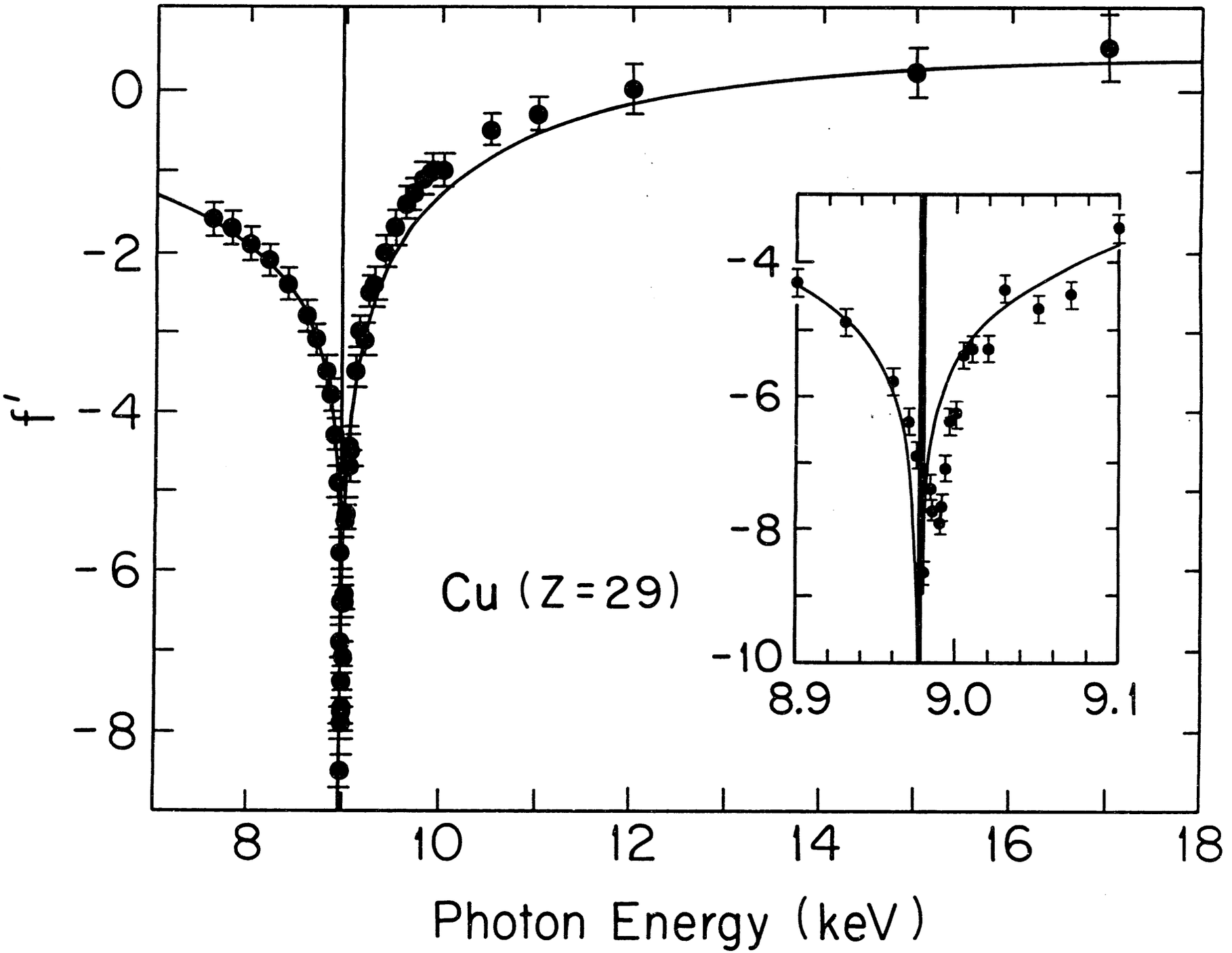

Fig. 6

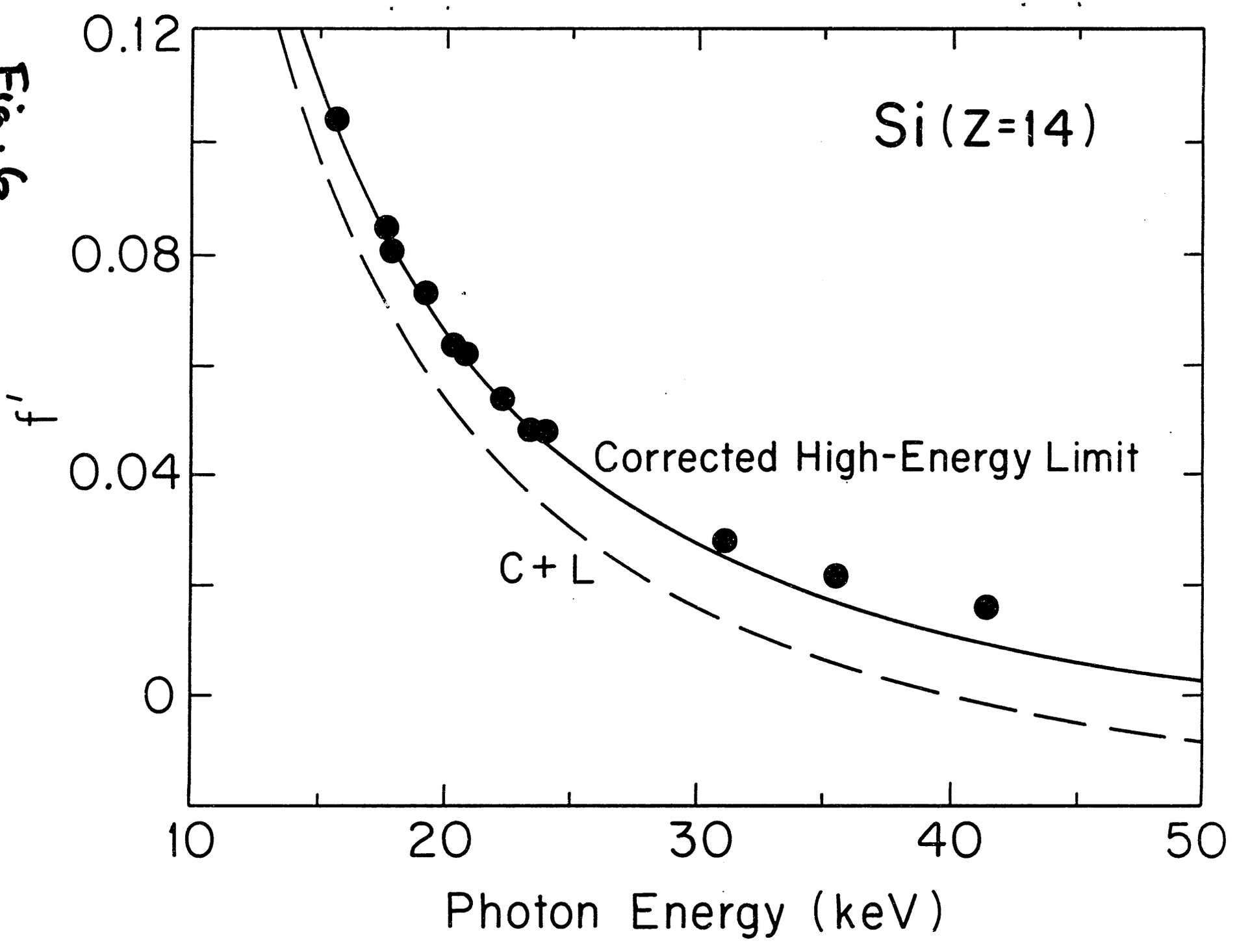
Si (Z=14)
Corrected High-Energy Limit
C + L
f'
0.12
0.08
0.04
0
10
20
30
40
50
Photon Energy (keV)

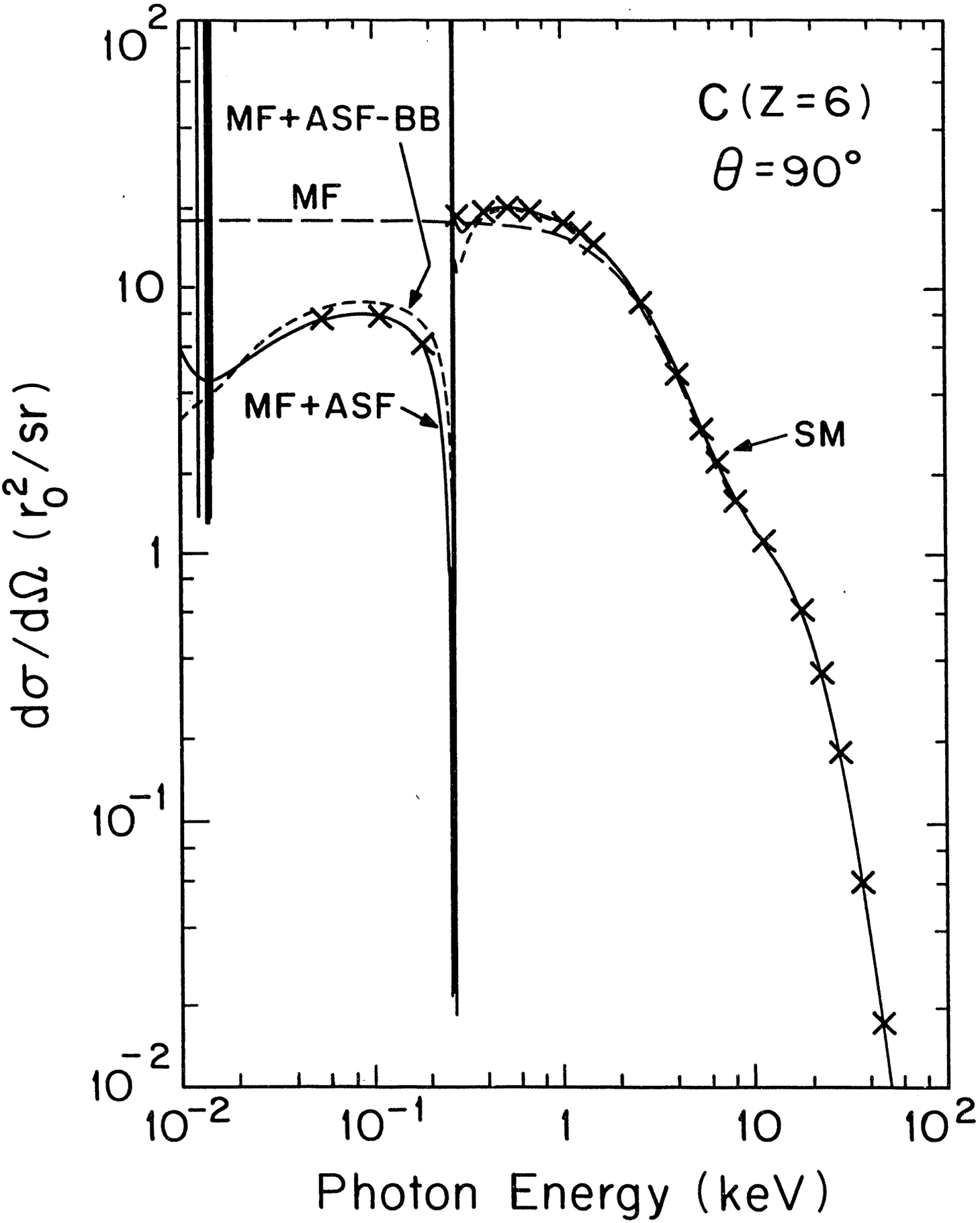
C (Z = 6)
θ = 90°
MF+ASF-BB
MF
MF+ASF
SM
dσ/dΩ (r₀²/sr)
Photon Energy (keV)
10²
10
1
10⁻¹
10⁻²
10⁻²
10⁻¹
1
10
10²

Fig. 7

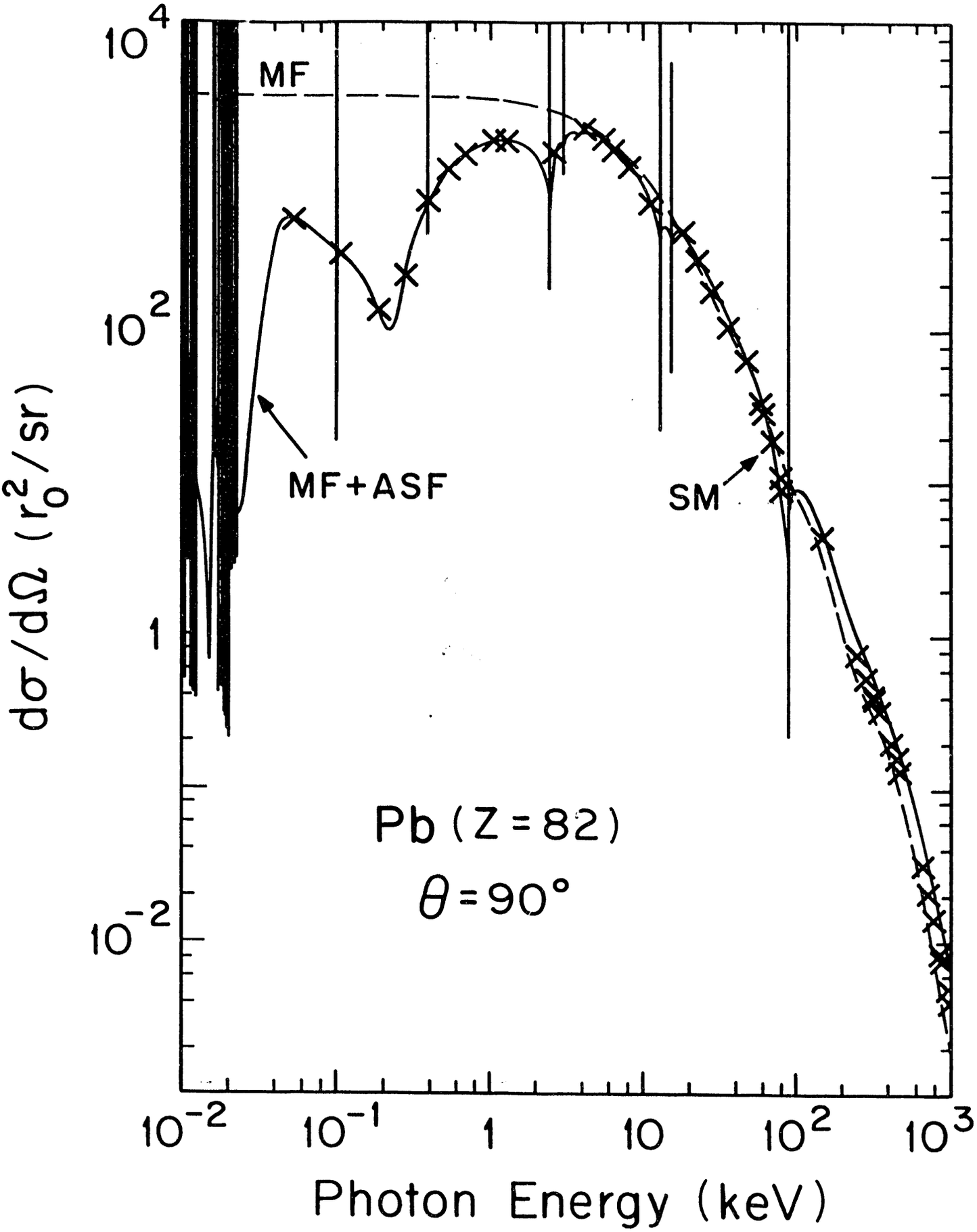
MF
MF+ASF
SM
Pb (Z = 82)
θ = 90°
dσ/dΩ (r₀²/sr)
Photon Energy (keV)
10⁴
10²
1
10⁻²
10⁻²
10⁻¹
1
10
10²
10³

Fig. 8

Fig. 9

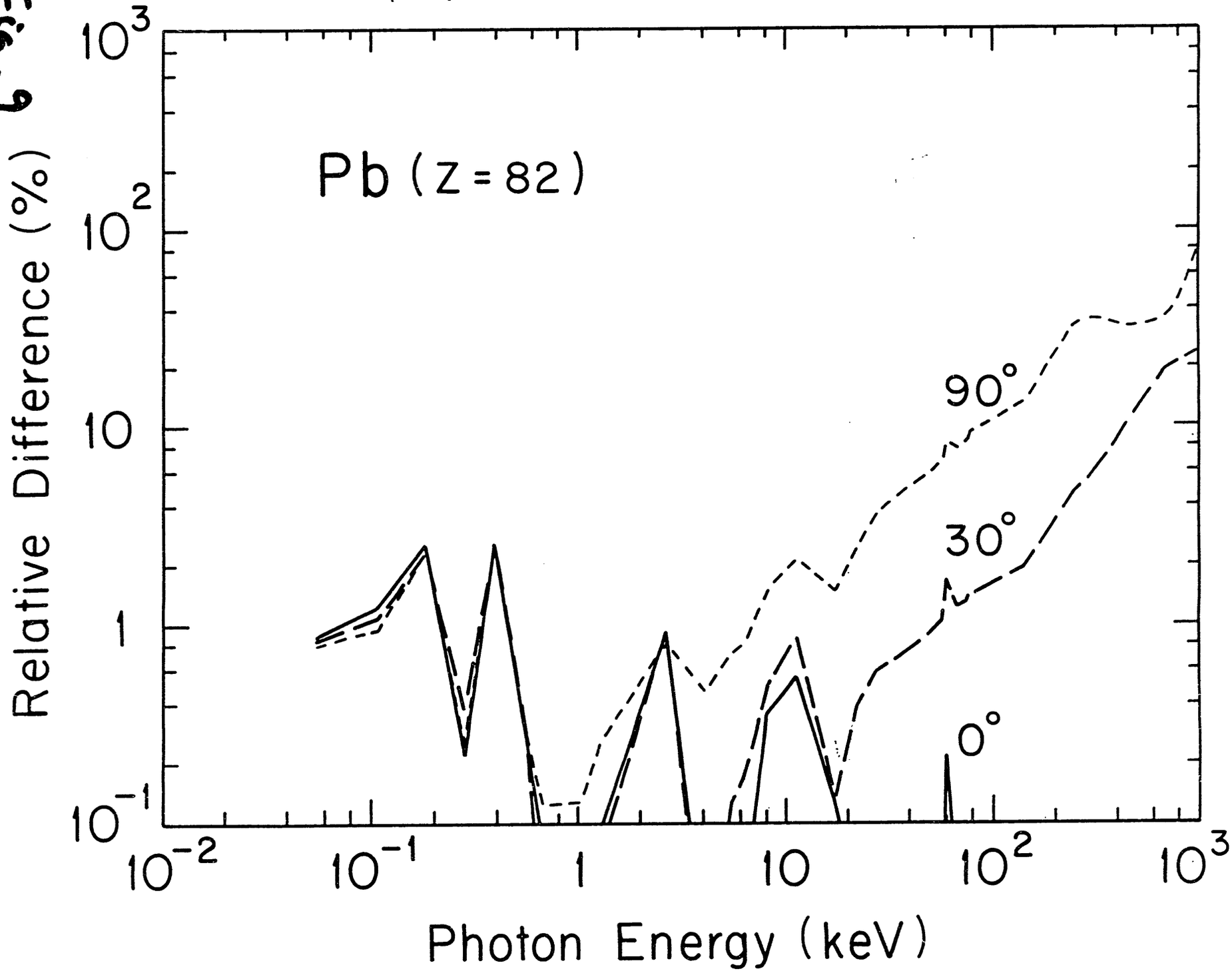
Pb (Z = 82)
90°
30°
0°
Relative Difference (%)
Photon Energy (keV)
10^3
10^2
10
1
10^{-1}
10^{-2}
10^{-1}
1
10
10^2
10^3

Fig. 10

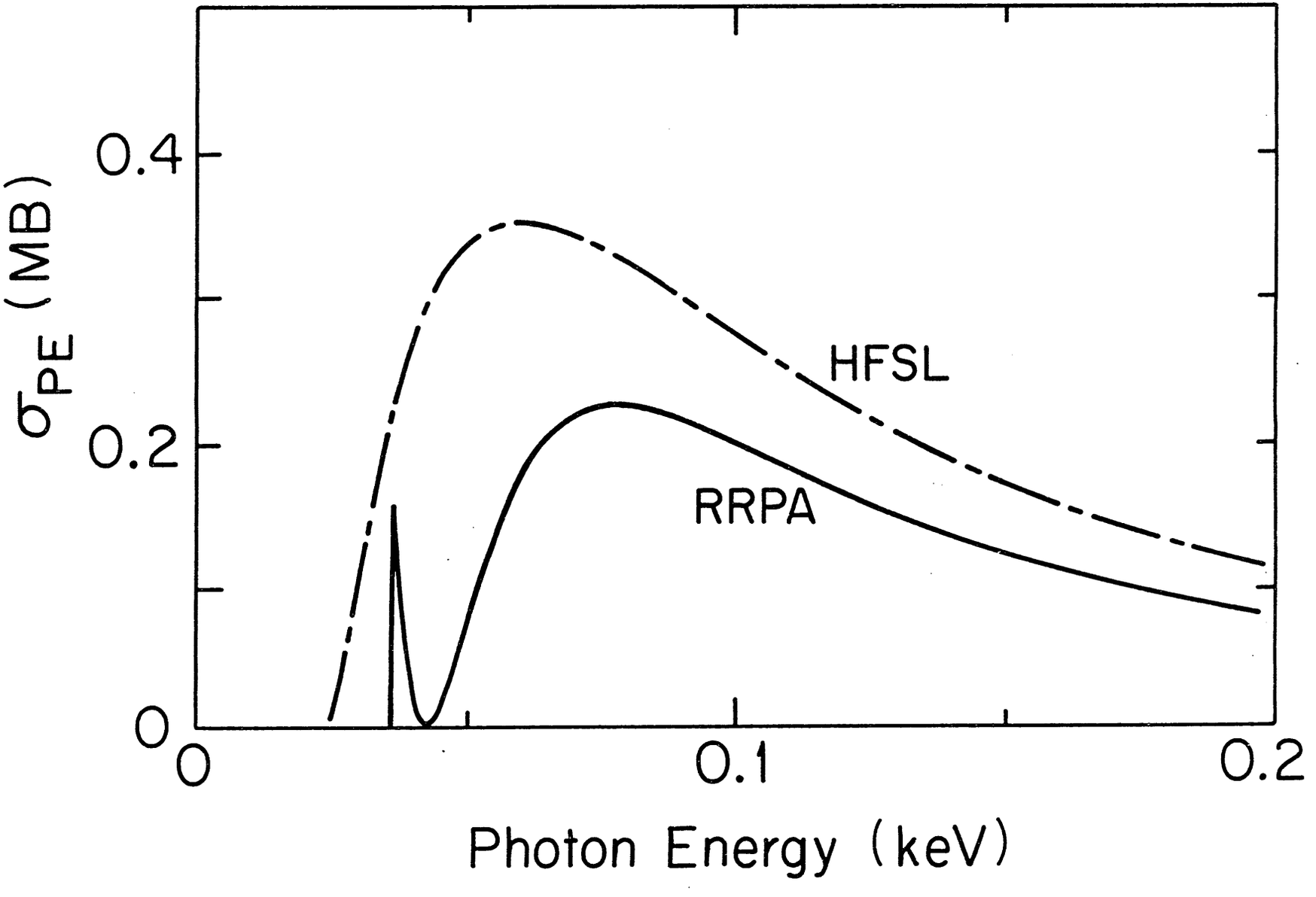

Fig. 11

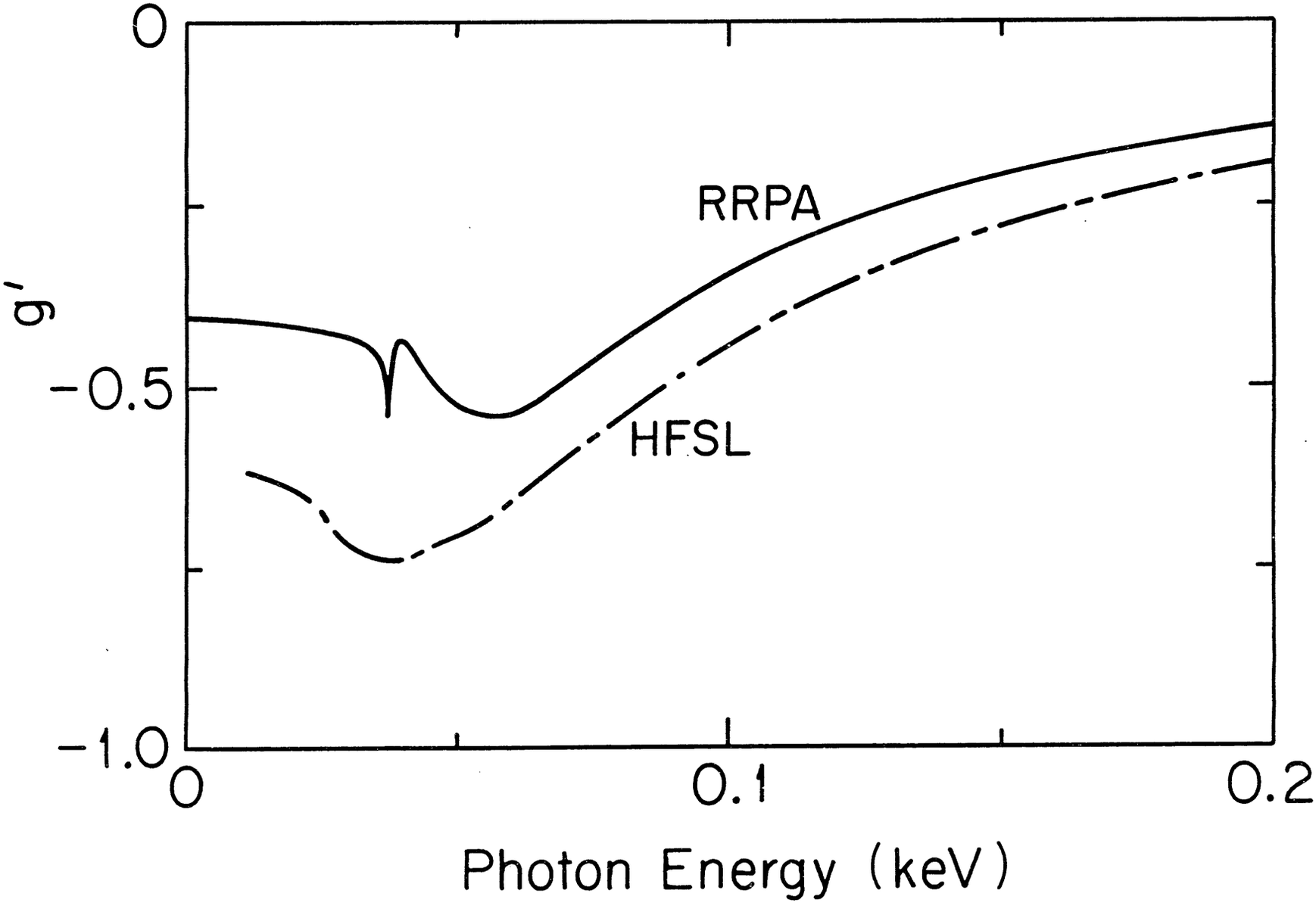

Fig. 12

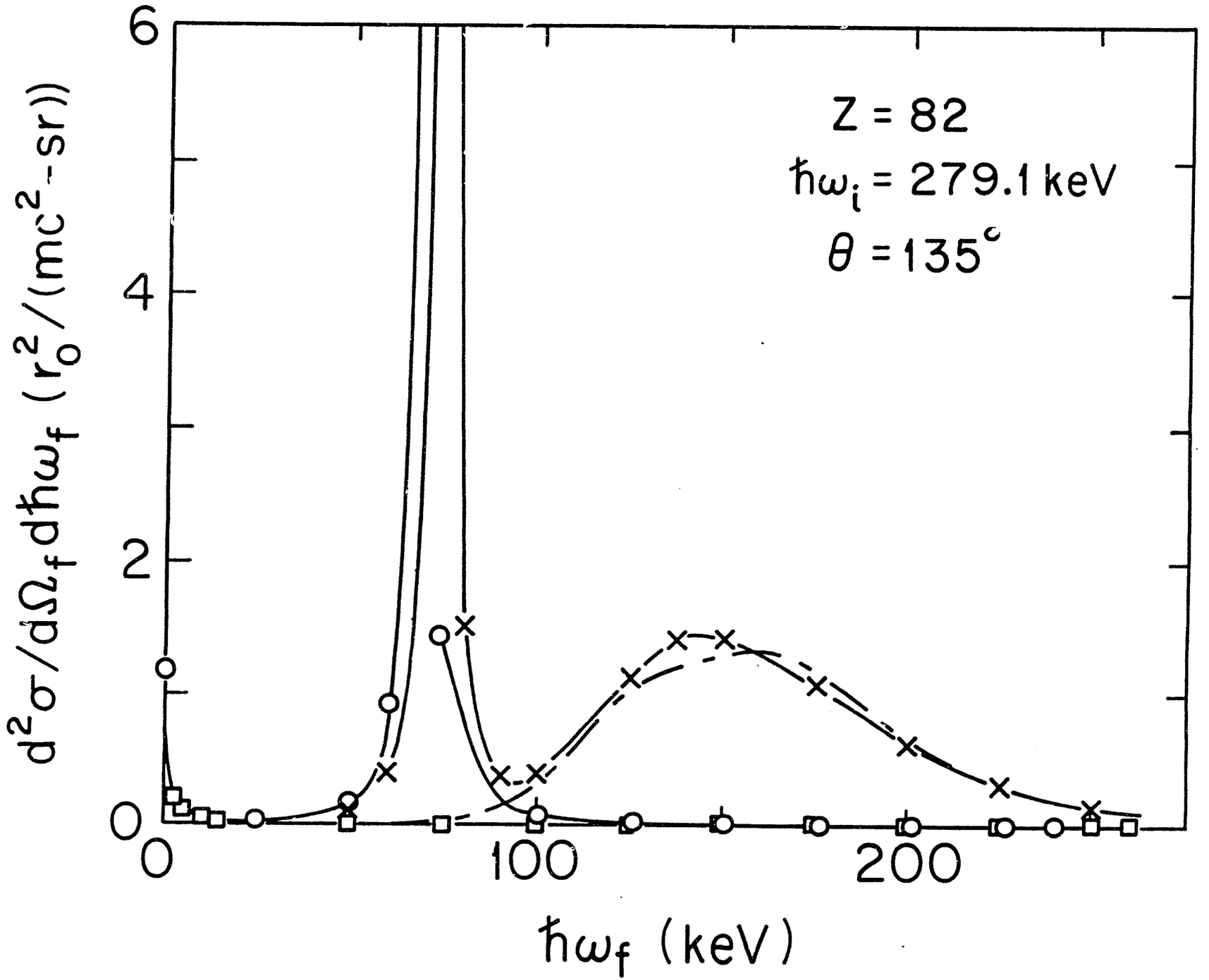
Z = 82
ħω_i = 279.1 keV
θ = 135°
d²σ/dΩ_f dħω_f (r_0²/(mc²-sr))
ħω_f (keV)
0
2
4
6
0
100
200

Fig. 13

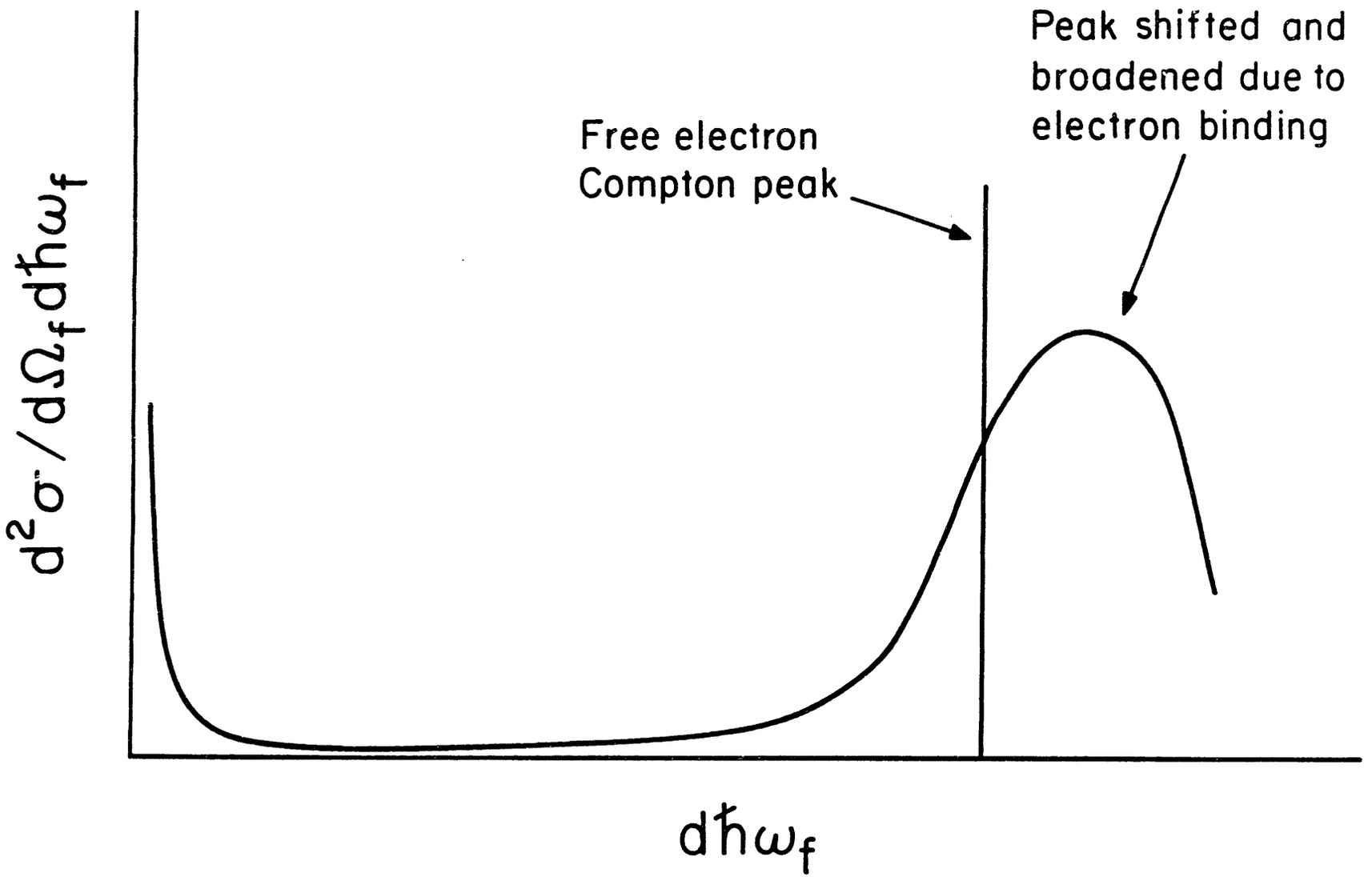
Peak shifted and broadened due to electron binding
Free electron Compton peak
$d^2\sigma/d\Omega_f d\hbar\omega_f$
$d\hbar\omega_f$

Fig. 14

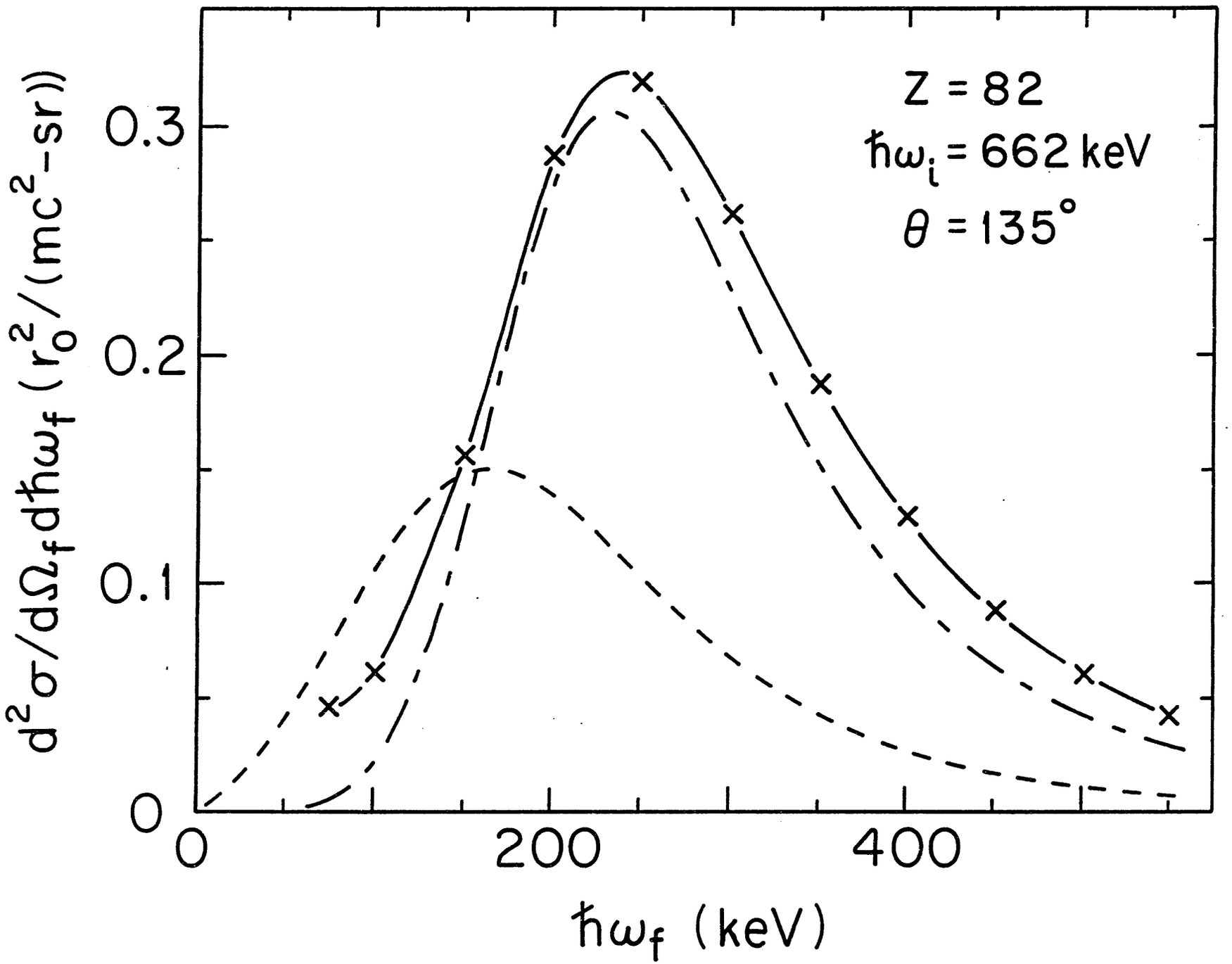
Z = 82
ħω_i = 662 keV
θ = 135°
0.3
0.2
0.1
0
0
200
400
d²σ/dΩ_f dħω_f (r_0²/(mc²-sr))
ħω_f (keV)

Fig. 15

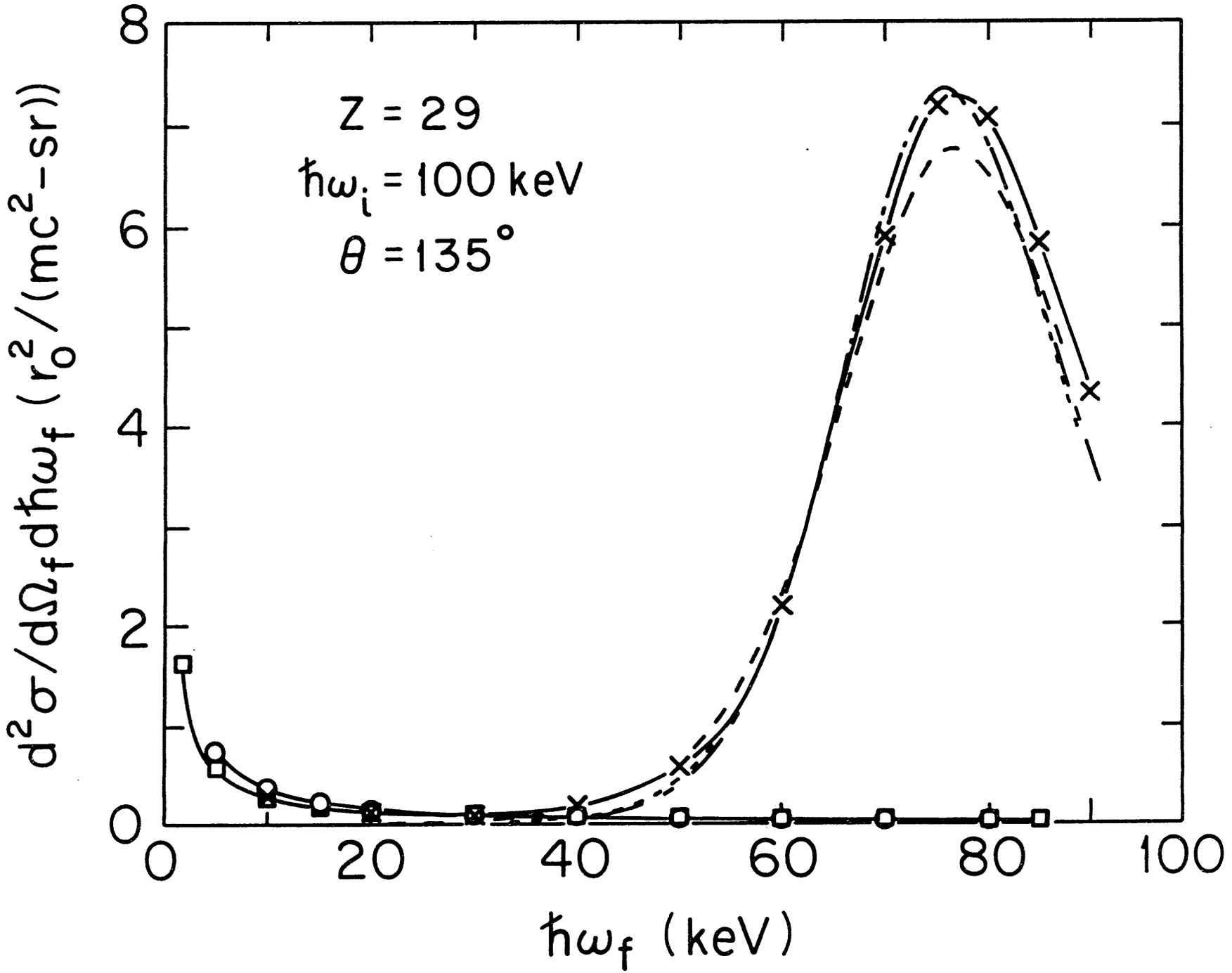
Z = 29
$\hbar\omega_i$ = 100 keV
θ = 135°
$d^2\sigma/d\Omega_f d\hbar\omega_f$ ($r_0^2/(mc^2$-sr))
$\hbar\omega_f$ (keV)
0
2
4
6
8
0
20
40
60
80
100

Fig. 16

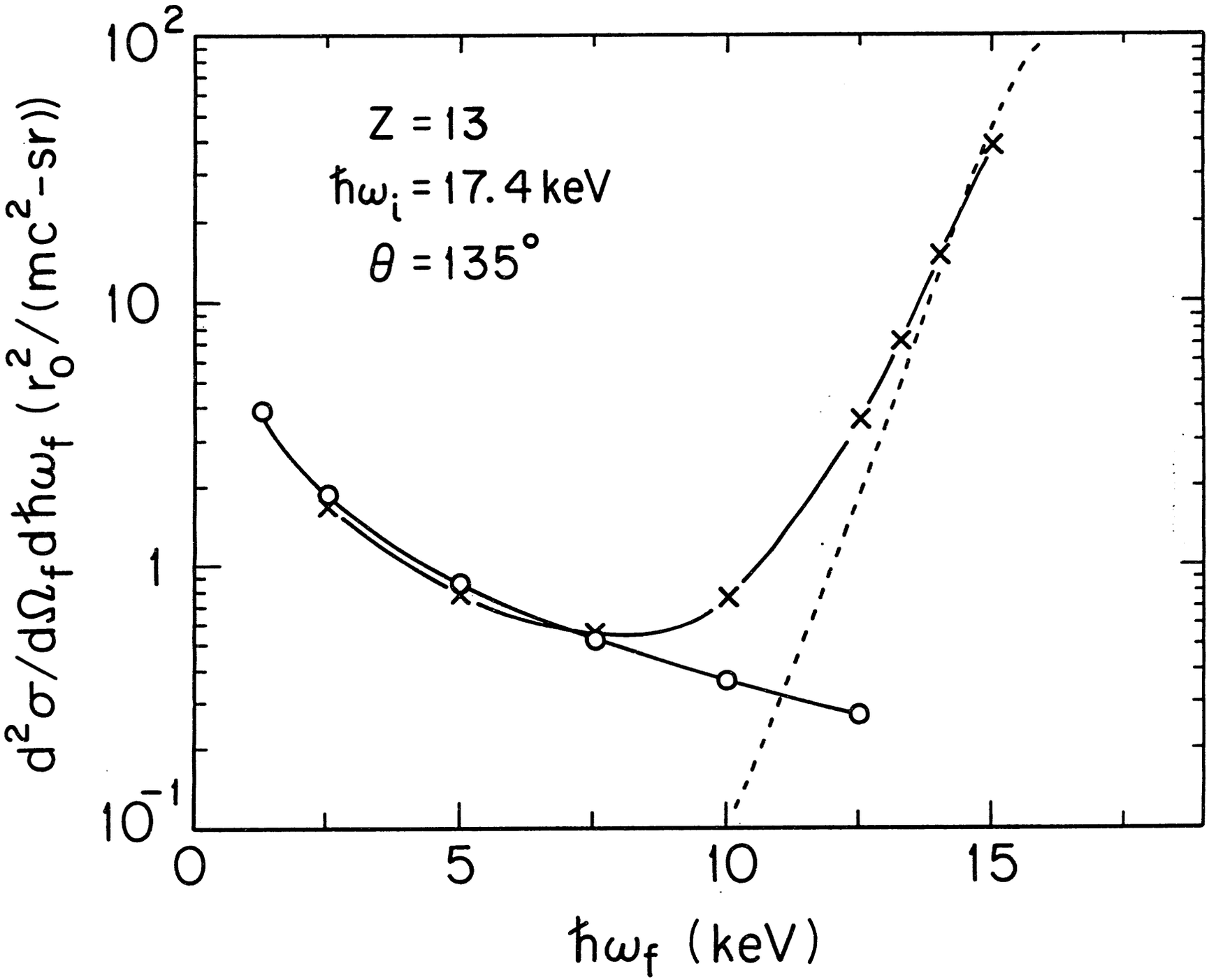
Z = 13
ħω_i = 17.4 keV
θ = 135°
10^2
10
1
10^-1
0
5
10
15
d²σ/dΩ_f dħω_f (r_0²/(mc²-sr))
ħω_f (keV)

Fig. 17

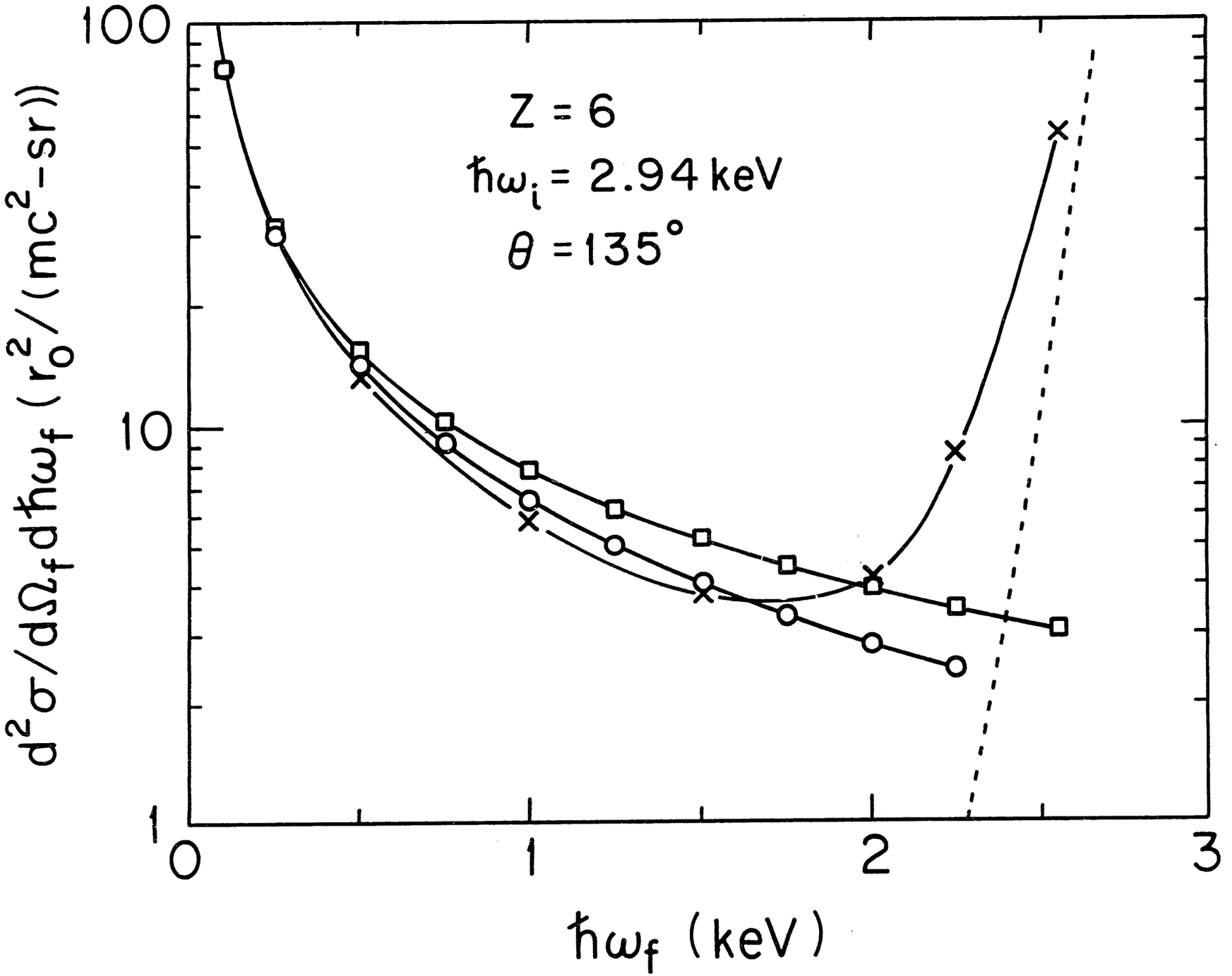

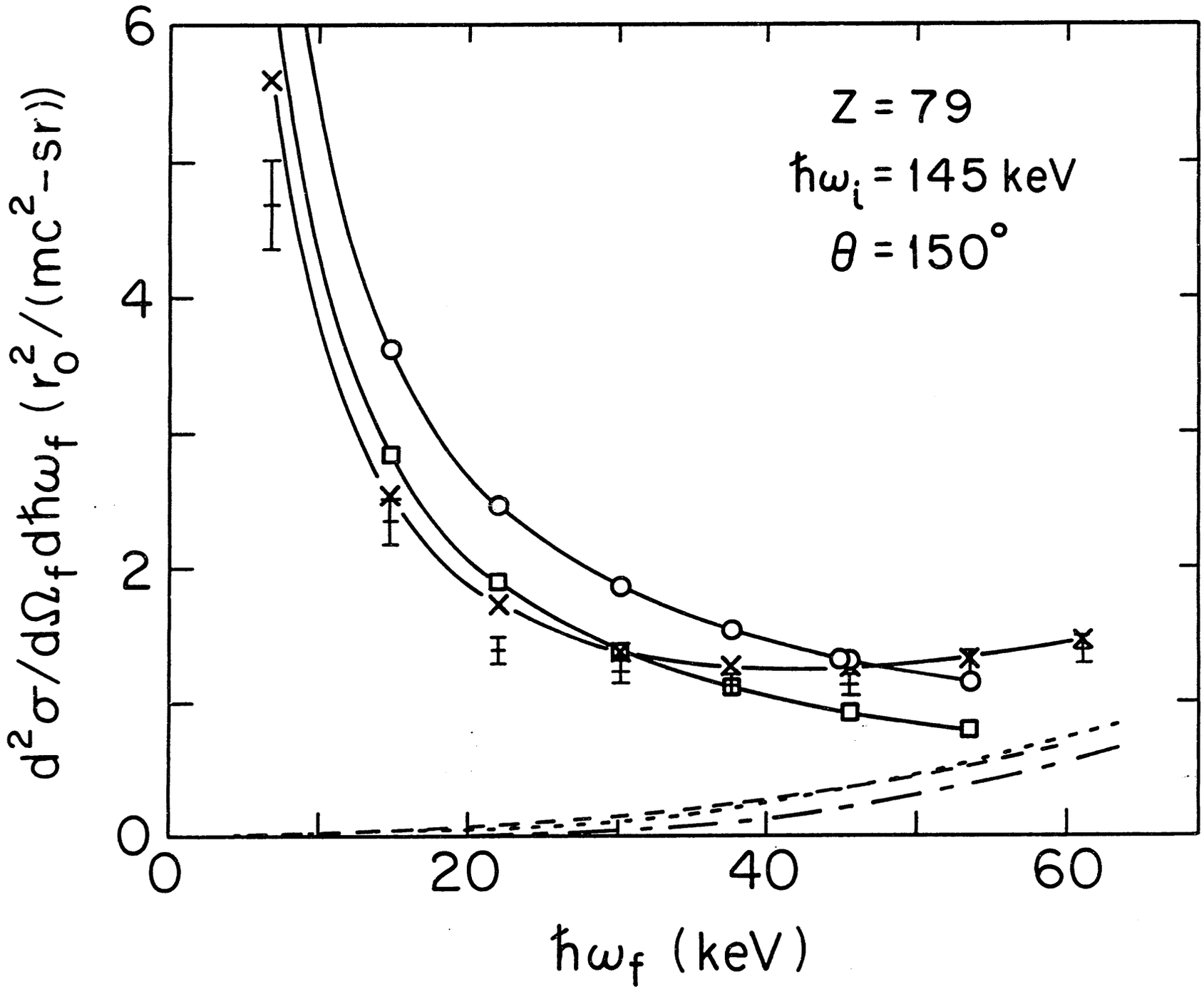
Z = 79
ħω_i = 145 keV
θ = 150°
d²σ/dΩ_f dħω_f (r_0²/(mc²-sr))
ħω_f (keV)
0
2
4
6
0
20
40
60

Fig. 18

Fig. 19

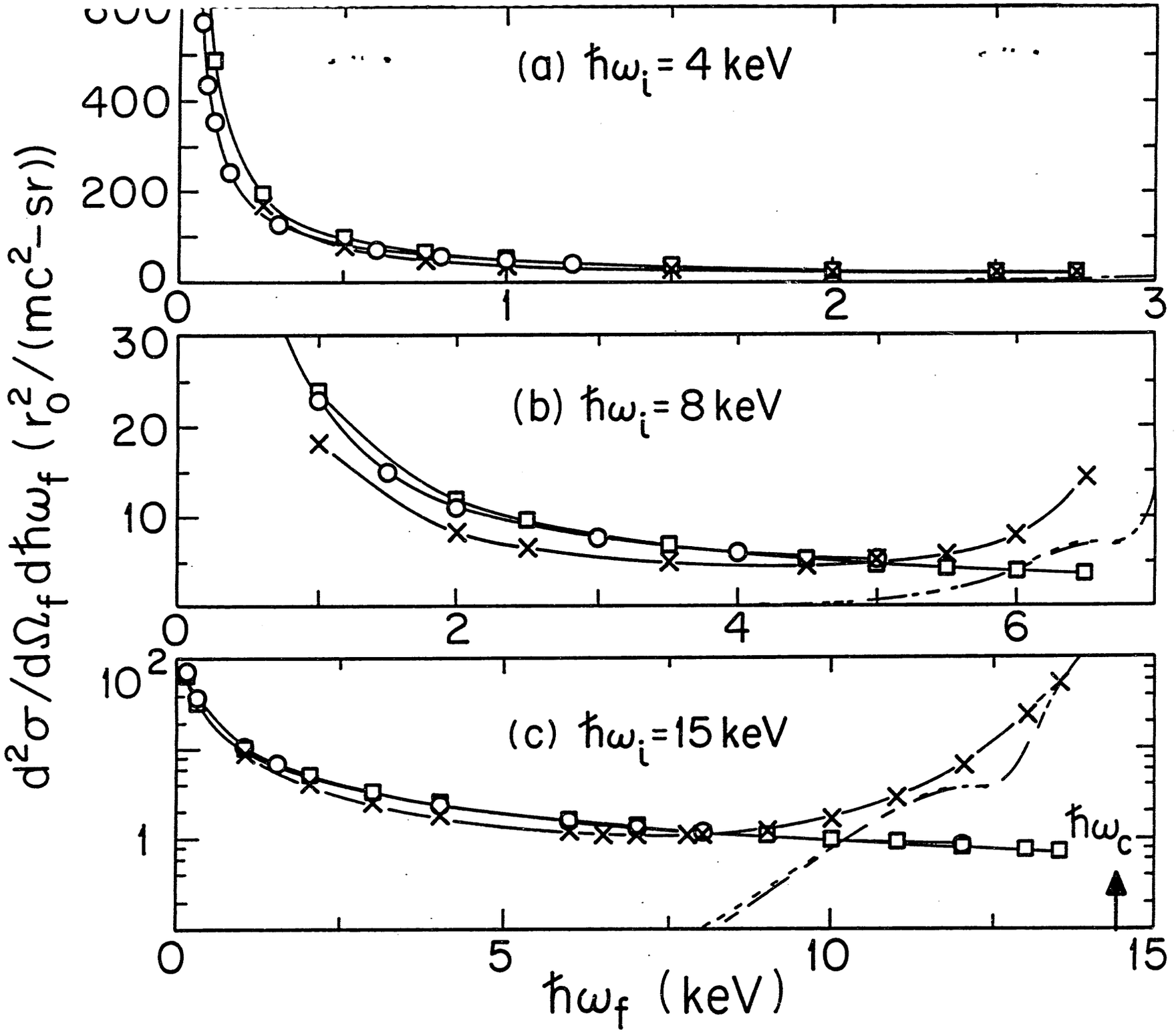
(a) $\hbar\omega_i = 4$ keV
(b) $\hbar\omega_i = 8$ keV
(c) $\hbar\omega_i = 15$ keV
$\hbar\omega_c$
$d^2\sigma/d\Omega_f d\hbar\omega_f$ ($r_0^2/(mc^2\text{-sr})$)
$\hbar\omega_f$ (keV)
0
200
400
1
2
3
10
20
30
4
6
10^2
5
15

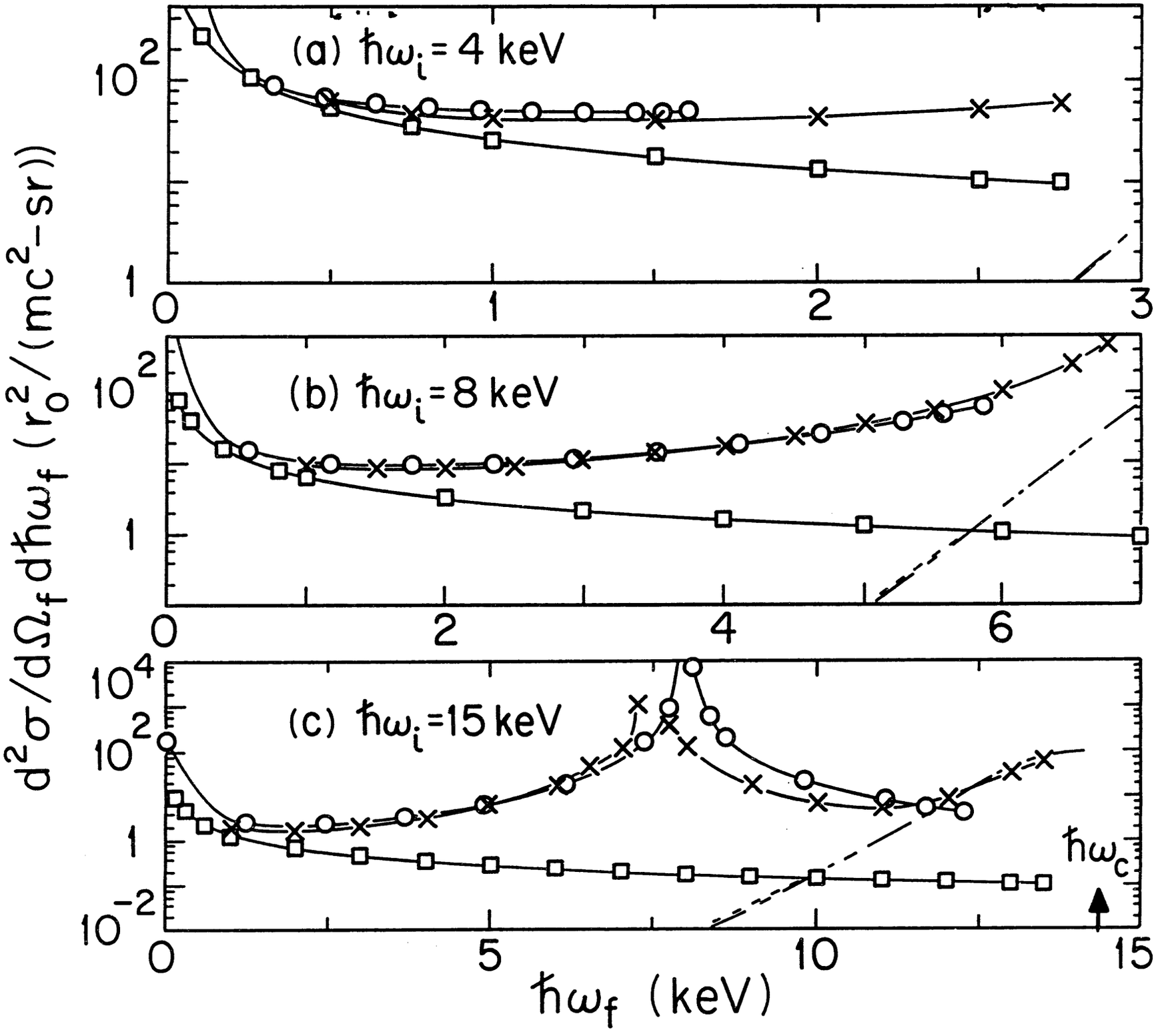
(a) $\hbar\omega_i = 4$ keV
(b) $\hbar\omega_i = 8$ keV
(c) $\hbar\omega_i = 15$ keV
$\hbar\omega_c$
$d^2\sigma/d\Omega_f d\hbar\omega_f$ ($r_0^2/(mc^2\text{-sr})$)
$\hbar\omega_f$ (keV)

Fig. 20

END

DATE FILMED

11/5/93